Yukon

MR-23-01

Predictive Wetland Mapping

Peel Watershed Planning Region, Yukon

September 2023

Predictive Wetland Mapping: Peel Watershed Planning Region, Yukon

Government of Yukon
Fish and Wildlife Branch
MR-23-01

Author[s]
WSP E&I Canada Limited

Copies available from:
Environment Yukon
Fish and Wildlife Branch, V-5
Box 2703, Whitehorse, Yukon Y1A 2C6
Phone (867) 667-5721
Email: environmentyukon@gov.yk.ca
Online: www.env.gov.yk.ca

Suggested citation:
WSP E&I CANADA LIMITED. 2023. Predictive Wetland Mapping: Peel Watershed Planning Region, Yukon (MR-23-01). Government of Yukon, Whitehorse, Yukon, Canada.

PREDICTIVE WETLAND MAPPING

PEEL WATERSHED PLANNING REGION, YUKON

GOVERNMENT OF YUKON

PROJECT NO.: CE05106
DATE: MARCH 2023

WSP E&I Canada Limited
5681 70 Street NW
Edmonton, AB T6B 3P6

T: +1 780-436-2152

WSP.com

31 March 2023

Nadele Flynn
Tyler Kuhn
Fish and Wildlife, Environment
Government of Yukon
10 Burns Road
Whitehorse, Yukon Y1A 4Y9

Dear Ms. Flynn and Mr. Kuhn:

Subject: Predictive Wetland Mapping, Peel Watershed Planning Region, Yukon

This report has been prepared for the Government of Yukon with specific application to the Predictive Wetland Mapping, Peel Watershed Planning Region, Yukon Project. This report with accompanying wetlands map is based on the satellite imagery collected in 2021 and the field data collected between 1975 and 2020.

Any use which a third party makes of this report, or any reliance on or decisions made based on it, are the responsibility of such third parties. WSP E&I Canada Limited (WSP) accepts no responsibility for damages, if any, suffered by any third party because of decisions made or actions based on this report. The work was conducted in accordance with the scope of work prepared for the Project, and generally accepted remote sensing and biological work practices. No other warranty, expressed or implied, is made.

Should you have any questions, please contact the undersigned at your earliest convenience.

Yours sincerely,

Rebecca Warren, M.Sc.
Remote Sensing and GIS Specialist

RW/cj

WSP E&I Canada Limited
5681 70 Street NW
Edmonton, AB T6B 3P6

T: +1 780-436-2152
wsp.com

QUALITY MANAGEMENT

ISSUE/REVISION	FIRST ISSUE	REVISION 1	REVISION 2	REVISION 3
Remarks		Updated to reflect report revisions requested by Government of Yukon	Updated to address edits/comments requested by Government of Yukon	
Date	March 31, 2022	March 10, 2023	30 March 2023	
Prepared by	Rebecca Warren	Rebecca Warren	Rebecca Warren	
Signature				
Checked by	Meisam Amani	Meisam Amani Deo Heeraman	Deo A Heeraman	
Signature				
Authorized by	Deo A Heeraman	Deo A Heeraman	Deo A Heeraman	
Signature				
Project number	CE05027	CE05106	CE05106	
Report number				
File reference				

EXECUTIVE SUMMARY

This report accompanies and discusses the mapping of wetland areas and adjacent non-wetland areas in the Peel Watershed Planning Region (PWPR) developed by WSP E&I Canada Limited (WSP) under contract with Government of Yukon. Wetland areas were classified according to the Canadian Wetland Classification System and include shallow water (less than 2 m deep), bogs, fens, marshes, and swamps. Non-wetland areas were identified as deep water (greater than 2 m deep), exposed/disturbed, coniferous forest, broadleaf forest, and shrubland. Wetlands were classified using an object-based Random Forest model in eCognition (version 10.1) using optical (i.e., Sentinel-2) and Synthetic Aperture Radar (i.e., Sentinel-1, ALOS PALSAR) satellite imagery, and topographic data (i.e., merged Canadian Digital Elevation Model and ArcticDEM). Model training and assessment data was acquired through previous field surveys and the interpretation of high-resolution satellite imagery (i.e., SPOT 6/7 and Esri World Basemap Imagery). The field survey data was acquired through various projects from 1975 to 2020 and could included information on vegetation, soil characteristics, landscape position, and landcover class. These data were available within the Yukon Biophysical Information System (YBIS). Interpreted sites were assigned a wetland or non-wetland class only. A polygon was manually delineated for each field and interpreted site and used as inputs for the segmentation and split two-thirds and one-third for training and assessing the Random Forest model. The classification was manually refined to correct errors, such as shadows in the input imagery being mapped as water, by changing an object's mapped class or altering object boundaries. The final classification was assessed visually and statistically for accuracy by Government of Yukon, WSP and First Nation of Na-Cho Nyak Dun. Based on the results, approximately 9% of the total area within the PWPR is comprised of wetlands. The overall wetland classification accuracy for wetland versus non-wetland areas was 92.46% (Kappa coefficient equals 0.85) and 79.85% (Kappa coefficient equals 0.64) for the five wetland classes. These results show that the approach used in this project offers great potential for wetland classification in future studies and will assist in management decisions related to land use planning and management of the PWPR.

TABLE OF CONTENTS

TABLES

FIGURES

APPENDICES

1 INTRODUCTION

Wetland mapping initiatives in Canada have increased in recent years leading to a plethora of scientific research and operational methodologies across a wide range of geographies, including Yukon. This is in part due to wetlands covering large portions of the landscape, their role in soil and water conservation, and susceptibility to disturbance, both anthropogenic and climatic. In addition, land use planning initiatives in Yukon in part rely on wetland maps to provide recommendations for research and management strategies for minimizing impacts to these sensitive ecosystems that will be relied on for industrial and traditional uses.

Remote sensing is the science of obtaining information about an object, area, or phenomenon by examining data acquired by a device that is not in contact with it. These devices can include, but are not limited to, satellites, aircrafts, and drones. Data is acquired by a sensor on the device that emits and/or observes how energy (i.e., electromagnetic radiation) interacts with the object, area, or phenomenon of study. Over the past 40 years, numerous satellites have been launched into orbit that provide valuable information for understanding earth processes, including wetlands. Satellites provide coarse to high spatial resolution and multispectral imagery over large areas, with minimal effort. Moreover, the availability of open-source datasets has greatly improved the efficiency and cost-effectiveness of mapping and monitoring earth systems at scale, benefitting researchers, land use planners, and policy makers. Previous wetland mapping studies completed with remote sensing technologies have established that a combination of optical, synthetic aperture radar (SAR), and topological data (e.g., Digital Elevation Models (DEM)) is the optimal technique to achieve the highest possible classification accuracy (Amani et al. 2017a, 2020; Mahdavi et al. 2018; Mahdianpari et al. 2021; Merchant et al. 2019, 2020). It has also been shown to be beneficial to derive additional features from the satellite data and include them in the classification, such as band ratios, indices, and elevation derivatives like slope, to assist in separating landcover classes. In regard to classification methodologies, it has been widely reported that an object-based classification method is superior to pixel-based techniques (Corcoran et al. 2015), especially for wetland mapping (Amani et al. 2017a, 2018b; Mahdavi et al. 2018), due to its ability to consider multiple data inputs (i.e., optical, SAR, and DEM images), capture class heterogeneity (e.g., form; graminoid, shrubby, wooded), and reduce noise (image artifacts not representing real world features), along with reported higher classification accuracies. In pixel-based classifications, each pixel is assigned a class based on that pixel's spectral properties without consideration of neighbouring pixels. However, in object-based image analysis (OBIA), pixels are grouped into objects based on spectral similarity or other external variables, such as soil or geological unit. OBIA additionally enables utilizing object spatial information and produces more proper results in terms of visual interpretations (Blaschke 2010).

Machine learning techniques have been extensively used in landcover classification where Random Forest (RF) models have yielded higher accuracies compared to other commonly used machine learning algorithms, such as Support Vector Machine, Maximum Likelihood, and K-Nearest Neighbours, for wetland classification (Amani et al. 2017a; Mahdavi et al. 2018). RF is a non-parametric classifier which contains an ensemble of decision trees each of which possess several nodes dividing the input objects into mutually exclusive groups. The division continues until each node is representative of one of the final classes (Breiman 2001), and the majority result of all trees determines the class label for a particular object. RF contains several tuning parameters that are selected based on various factors, such as the number of samples, tree depth, and number of trees. A similar approach to mapping wetlands was undertaken by Ducks Unlimited Canada for the Dawson Regional Landuse Plan. Mahdavi et al. (2018)

additionally provides an extensive overview of remote sensing for wetland classification beyond what is discussed in this report.

1.1 PROJECT BACKGROUND

In August of 2019, the Tr'ondëk Hwëch'in, First Nation of Na-cho Nyäk Dun, Vuntut Gwitchin Government, Gwich'in Tribal Council, and the Government of Yukon approved a regional land use plan for the Peel Watershed Planning Region. Part of the land use plan strategy is to provide recommendations for research and management strategies for minimizing impacts to the region's wetlands, including a survey of wetlands in the Peel region prior to any new major developments occurring. Currently, the region has no permanent residents, few roads, and limited development, with only 20% of the watershed open to future development, making the planning region one of the few remaining pristine watersheds in the world.

This report accompanies and discusses the mapping of wetland and adjacent non-wetland areas in the Peel Watershed Planning Region. The mapping was completed using the object-based machine learning algorithm Random Forest with multiple remote sensing datasets (i.e., Sentinel-2, Sentinel-1, ALOS PALSAR) and a DEM. The software eCognition Developer (version 10.1) was selected for use for this project as it is regarded as one of the best software for object-based classifications due to its ability to incorporate various types of datasets, provide a wide range of segmentation algorithms, incorporate variables such as shape, colour, texture, and contextual information in the model, and allow for the development of a knowledge base for the classification. Model training and assessment data acquired from a variety of previous field surveys completed between 1975 and 2020 and through image interpretation. Wetland areas were classified according to the five major wetland classes of the Canadian Wetland Classification System (CWCS; National Wetlands Working Group 1997) and include shallow water (less than 2 m deep), bogs, fens, marshes, and swamps. Non-wetland areas included deep water (greater than 2 m deep), exposed/disturbed, coniferous, broadleaf, and shrubland. Exposed/disturbed encompassed rock, gravel, sand and other similar landcovers that were either entire barren or with sparse vegetation. This class also included the little anthropogenic disturbance present in the watershed. The coniferous, broadleaf, and shrubland classes consist of landcovers of their respective dominant vegetation communities.

1.2 WETLAND CLASSIFICATION

Wetlands are defined by CWCS as areas that have been saturated for a prolonged period of time as to promote wetland processes as indicated by wet-adapted vegetation and hydric soils (National Wetlands Working Group 1997). The CWCS classifies wetlands into shallow water, marshes, fens, bogs, or swamps based on the characteristics of the vegetation communities and hydrology (Environment Yukon 2019; National Wetlands Working Group 1997). Shallow water systems have a water depth of less than two metres, and typically support multiple vegetation species, such as pond-lily and submerged aquatic vegetation. Marshes often form the transition between shallow water and the shoreline, and support rushes and sedges depending on water level fluctuations (Figure 1h). Swamps are periodically inundated, and the length and frequency of flooding influences the vegetation community (Figure 1i, j). Swamps can be shrub, coniferous, or broadleaf-dominated or a mixture of all three. Fens (Figure 1a, c, e, g) and bogs (Figure 1b, d, f) are peat-forming systems that support mosses, stunted vegetation, and ericaceous shrubs, and can additionally be characterized by hummocks or tussocks.

(a) Graminoid Fen

(b) Graminoid Bog

(c) Shrubby Fen

(d) Shrubby Bog

(e) Wooded, coniferous Fen

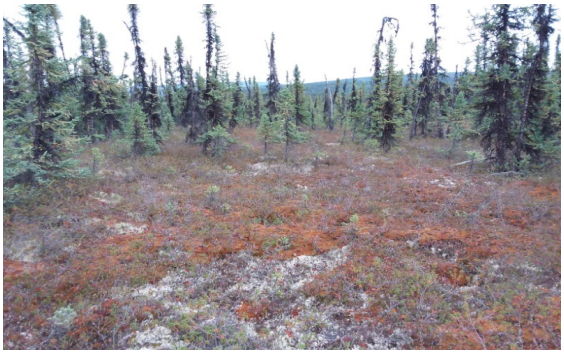

(f) Wooded, coniferous Bog

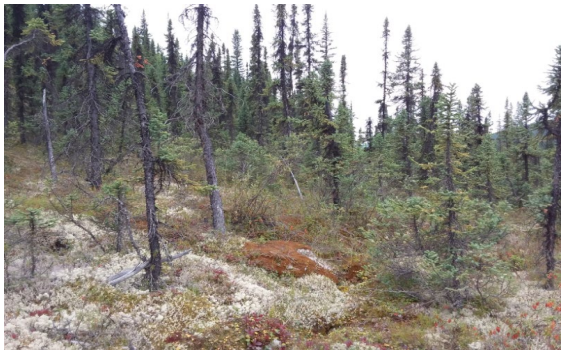

(g) Wooded, coniferous Fen

(h) Graminoid Marsh

(i) Shrubby Swamp

(j) Wooded, coniferous Swamp

Figure 1: Photos of field sites, collected by WSP in August 2021, representing some of the wetland forms found within the Mayo and McQuesten watersheds, Yukon, south of the Peel Watershed Planning Region

While large wetland complexes are most commonly found on level terrain, due to the permafrost conditions wetlands in Yukon can also occur on northern aspects and riparian drainages of various elevation and slope (Figure 1g). This is the result of frozen ground conditions impeding near-surface soil drainage, promoting the establishment of the wet-adapted vegetation and altered soils which characterize wetlands (National Wetlands Working Group 1997). Thermokarst wetlands, formed from a degradation in the underlying permafrost, are also present (Figure 1b). Additionally, in Yukon, peat deposits with a depth greater than 30 cm are considered peatlands if other indicators are present (CryoGeographic Consulting 2018; Environment Yukon 2019) as opposed to the greater than 40 cm depth cut-off described in the CWCS (National Wetlands Working Group 1997).

1.3 STUDY AREA

The Peel Watershed Planning Region (PWPR) is located in north-eastern Yukon and covers an area of 67,431 km^2 (Figure 2). The watershed falls within the Taiga Cordillera, Taiga Plains, and Tundra Cordillera ecoregions (Ecological and Landscape Classification of Ecoregions Technical Working Group, 2014; see https://map-data.service.yukon.ca/GeoYukon/Biophysical/Ecoregions_2014_1M), with large wetland complexes found throughout the northern half of the planning region. Permafrost is continuous throughout the watershed.

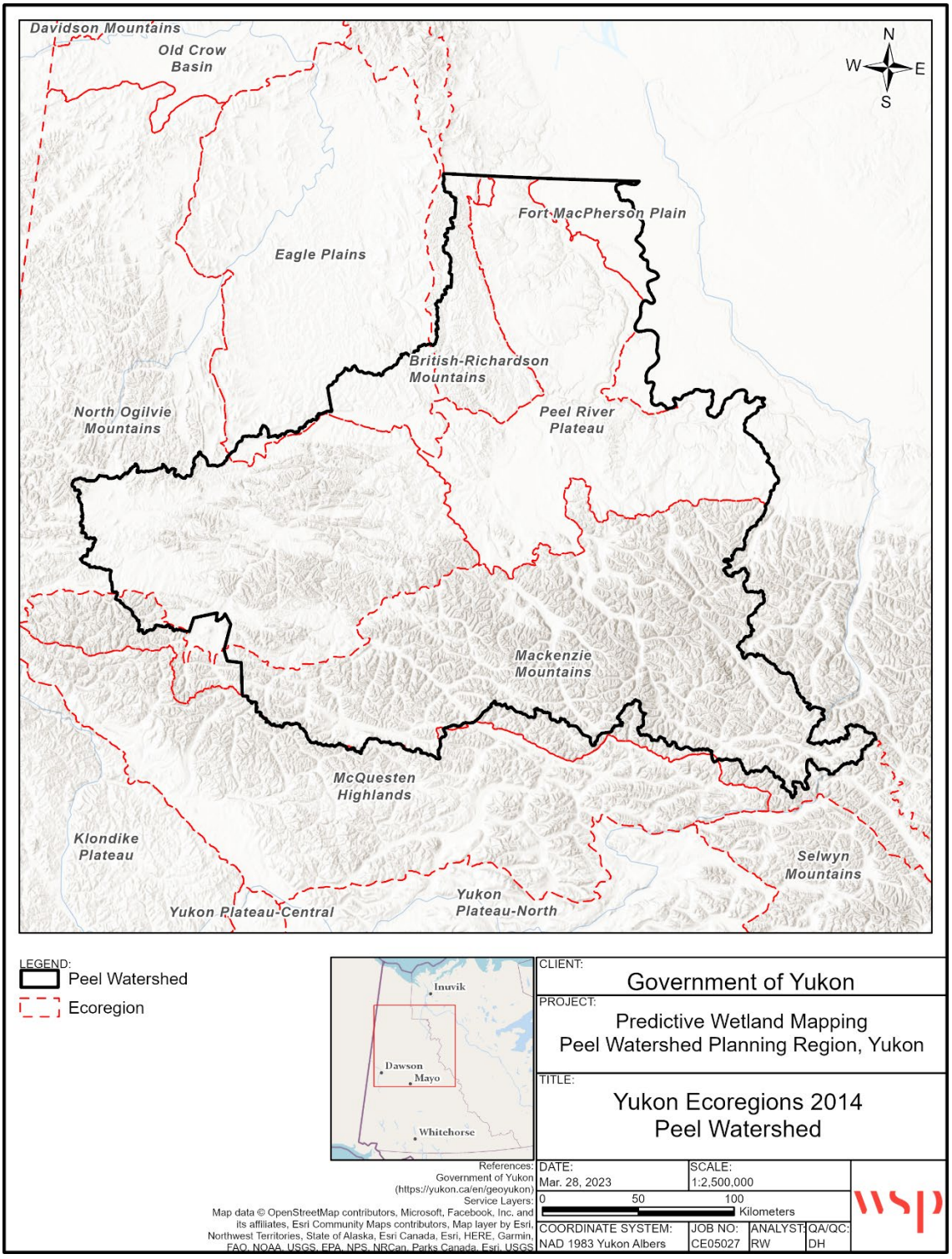

Figure 2: Ecoregions within the Peel Watershed Planning Region

The Taiga Cordillera ecozone covers the majority of the PWPR with mean annual temperatures ranging from -10°C to -4.5°C with annual precipitation ranging from 300 mm to >700 mm depending on location (Yukon Ecoregions Working Group 2004, p. 95-156). Open woodlands of white and black spruce, birch, willow, mosses, and lichen characterize the southern and lower elevation portions of the ecozone, with dwarf shrubs, mosses, lichens, saxifrages and mountain avens occurring at higher elevations. The Mackenzie Mountains ecoregion is located in the most southern portion of the PWPR and is characterized by landforms associated with multiple glaciations and extensive weathering. In contrast, the North Ogilvie Mountains ecoregion, situated in the western-most region of the PWPR, has not experienced glaciation in the recent past resulting in bare, flat-topped hills, with hummocky terrain or tussock tundra commonly occurring in valley bottoms. Only a small portion of the Eagle Plains ecoregion is covered by the PWPR, and like the North Ogilvie Mountains was not glaciated in the recent past. The Eagle Plains ecoregion is characterized by lower relief topography with black spruce woodlands and shrub tundra. The Peel River Plateau ecoregion, as redefined by Ecological and Landscape Classification of Ecoregions Technical Working Group (2014), is characterized by wetlands complexes, extensive burns, and ice-rich continuous permafrost (Yukon Ecoregions Working Group 2004, p. 75-82).

The Taiga Plains ecozone is represented by the Fort McPherson Plain ecoregion in the northeast and crosses into the Northwest Territories (Yukon Ecoregions Working Group 2004, p. 73-94). Mean annual temperature and precipitation is reported as -8°C and 300 mm, respectively. The region is characterized by low relief, low elevation topography as the result of past glaciation, and hosts extensive wetland complexes. It is estimated that approximately 25% of the ecoregion is covered in peatlands. Open black spruce – lichen forests dominate and host an understory of willow, shrub birch, Labrador tea, blueberry, and bog cranberry.

The Tundra Cordillera ecozone is represented by the British-Richardson Mountains ecoregion in the northwest portion of the PWPR (Ecological and Landscape Classification of Ecoregions Technical Working Group, 2014), which contain the largest extent of unglaciated mountain ranges in Canada (Yukon Ecoregions Working Group 2004, p. 97-106). Mean annual temperature falls around -7.5°C and precipitation ranging between 250 mm and 400 mm. Vegetation cover is heavily influenced by aspect and elevation and is dominated by shrub tundra. Trees are limited to lower elevation river valleys with favourable aspects, and shrub thickets occurring along shorelines or drainages.

2 DATASETS

2.1 FIELD SURVEY AND INTERPRETED DATA

The Ecological Inventory for the PWPR is a compilation of various projects conducted within the Peel Watershed between 1975 to 2020 which is available from the Government of Yukon's Yukon Biophysical Information System (YBIS; Yukon Government 2022). Vegetation field data was collected within plots and is contained in two files, plot listing and vegetation cover listing. Following the CWCS model, wetlands were classified into five broad classes (i.e., bog, fen, swamp, marsh, and shallow water) within the plot listing data file; however, the biophysical data recorded required further review to ensure the correct wetland class had been identified. Soil field data was also collected in conjunction with vegetation plots and is contained in two large files, soil listing and soil horizon listing. Soil types were classified based on the Canadian System of Soil Classification (CSSC) (Soil Classification Working Group 1998) and included information on Soil Order, Great Group, Sub-Group. Other soils information included terrain type, soil drainage, water source, water table depth, seepage depth, bedrock depth, rooting depth, and soil horizon characteristics including colour, texture, structure, mottles, presence of roots, stone content, coarse fragments, soil pH (mineral, organic), samples, mineral and permafrost soil depths. Soils information was used in conjunction with the vegetation information to verify wetland classes.

In total, 762 YBIS plots were distributed within the PWPR with most of the plots located in the southeast and northern regions, and few plots in the eastern and central regions (Figure 3). After initial review, 626 plots had adequate soils and vegetation information to determine a wetland (280 sites) or non-wetland (346 sites) class. An additional review was conducted to delineate representative site polygons for model training and assessment, which found that several YBIS plots did not have GPS location information that allowed for the confident identification of individual sites. For example, one location could represent multiple different plots. Where possible, individual plots were moved to a nearby representative location identified through the interpretation of satellite imagery. If a nearby representative area could not be confidently determined, the plot was excluded. Overall, 529 YBIS plots were used in model training and assessment which are summarized in Table 1. The GPS locations for the YBIS data were then used to manually delineate polygons representative of the assigned class at a scale of 1:10,000 for use in the OBIA. This scale was chosen based on mapping scale recommendations in Environment Yukon (2016, p. 21) for local ecosystem mapping.

Table 1: Summary of the Data Used to Train and Assess the Object-based Random Forest Model Acquired from the Yukon Biophysical Inventory System Database (1975 to 2020) and Interpreted from Satellite Imagery

CLASS	YBIS SITES		INTERPRETED SITES	
	NUMBER OF SITES	AREA (km²)	NUMBER OF SITES	AREA (km²)
Deep water	1	0.17	9	1.61
Exposed/disturbed	116	7.13	71	17.17
Coniferous forest	89	1.61	112	12.46
Broadleaf forest	5	0.12	15	1.14
Shrubland	131	3.30	46	4.68
Shallow water	7	0.07	17	0.60
Marsh	22	0.20	21	0.38
Fen	82	1.43	162	13.71
Bog	34	0.34	106	4.43
Swamp	42	0.28	49	1.70

Total	**529**	**14.65**	**608**	**57.88**

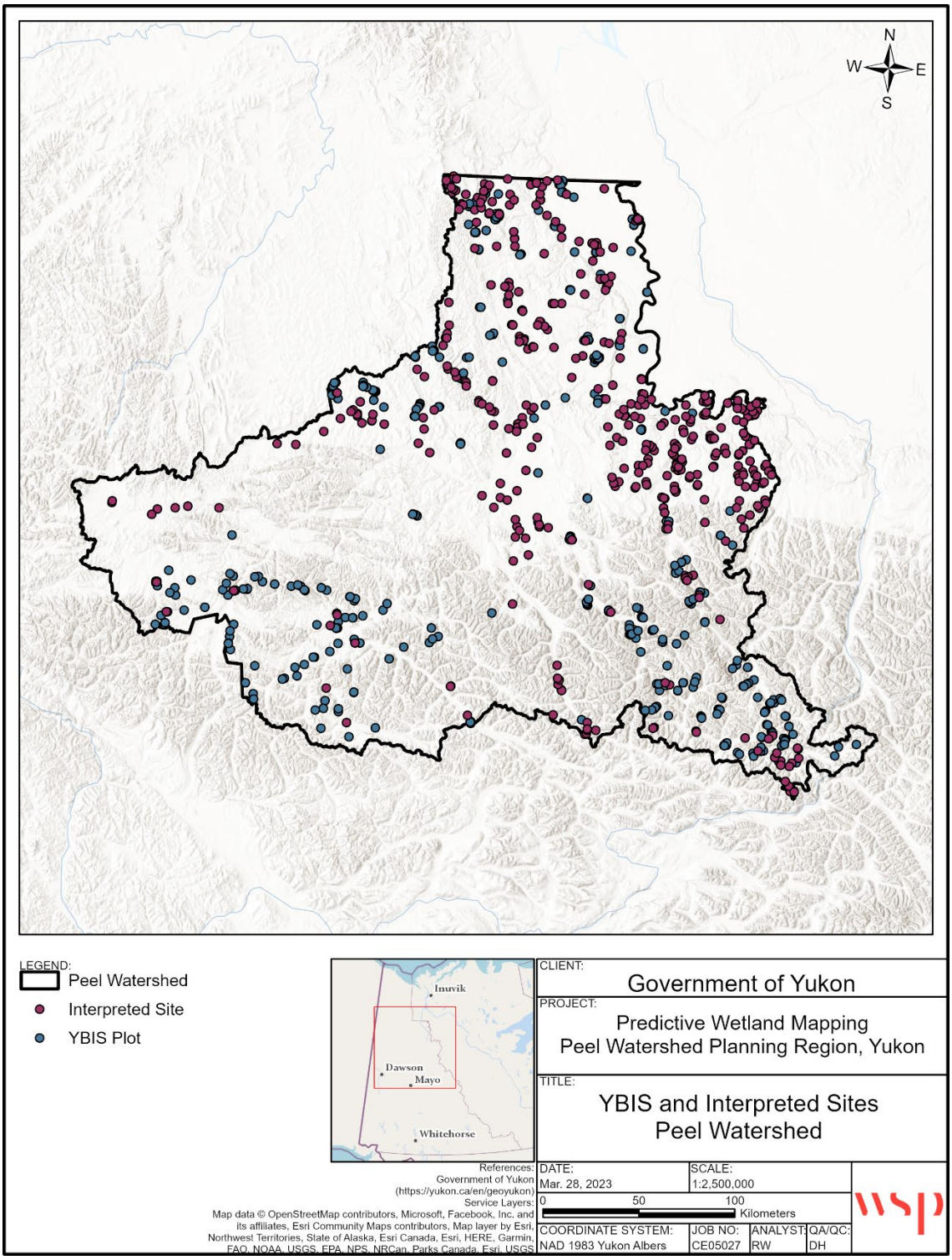

Figure 3: Overview map of the location of YBIS plots and satellite-interpreted polygons within the Project Area used for classification training and assessment of the wetland classification

Additional polygons were manually delineated and interpreted from high-resolution satellite imagery available through Government of Yukon (SPOT 6/7) and Esri (World Imagery Basemap) by an experienced remote sensing analyst. The predictive ecosystem mapping of the Peel Watershed (Meikle and Waterreus 2008) and the Soil Landscapes of Canada (White et al. 1992) datasets were also used as supplemental interpretation information. Interpreted sites were assigned a landcover class (i.e., classes listed in Table 1) based on spectral signature, general vegetation, and landscape position. For example, in high resolution imagery bogs typically appear as sparse treed forests with a mix of white (lichen) and orange (Sphagnum) coloured ground covers. In a Sentinel-2 imagery false colour composite, where the Red channel represents the NIR band, Green represents the SWIR1, and Blue represents the Red band, bogs typically appear bright pink (high Sphagnum coverage) to violet-brown (lichen and spruce). Care was taken to only select interpreted sites where the analyst had high confidence in the call based on a variety of the aforementioned characteristics and avoided fuzzy wetland boundaries to promote spectral purity in the training and assessment data. However, swamps and shallow water can be difficult to interpret from satellite imagery with certainty due to at times being unable to see the key indicators of these classes (e.g., water depth, hummocky ground, gleyed soils). In total, 608 additional sites were interpreted (Table 1, Figure 3).

During the segmentation processes, discussed later in this report (see section 3.1), the segmentation algorithm was parameterized to create segments that perfectly aligned with the delineated polygons to ensure no segments were used to train the model that were not within the manually delineated boundaries and to avoid boundary misalignment due solely to the difference in spatial resolution (i.e., boundaries visible in 1.5 m SPOT imagery versus 10 m Sentinel-2 imagery). However, the segmentation algorithm was not prevented from subdividing the input polygons into smaller segments, thus a delineated polygon could contain multiple segments. This allowed the segmentation process to identify site heterogeneity (e.g., separate inundated versus vegetated portions of a patterned fen), and provided a range of class spectral variance for the model to be trained on. The finer segmentation scale additionally increased the number of training polygons used in model training and addressed the variance in the size of the delineated site polygons (i.e., by subdividing into smaller segments based on a scale parameter). Field and interpreted polygons were combined and randomly split two-thirds training and one-third assessment per class. In total 1,138 sites were used for model training and assessment (Table 1).

2.2 SATELLITE DATA

It is well accepted that the fusion of optical, SAR, and DEM data is the optimal combination for wetland mapping with the highest possible classification accuracy (Mahdavi et al. 2018). In this project, Sentinel-2, Sentinel-1, ALOS PALSAR, and DEM data (Figure 4) were the primary inputs applied to classify wetlands in the PWPR. A brief description of each dataset and the related processing is provided in the following subsections. A full list of imagery used is presented in Appendix A.

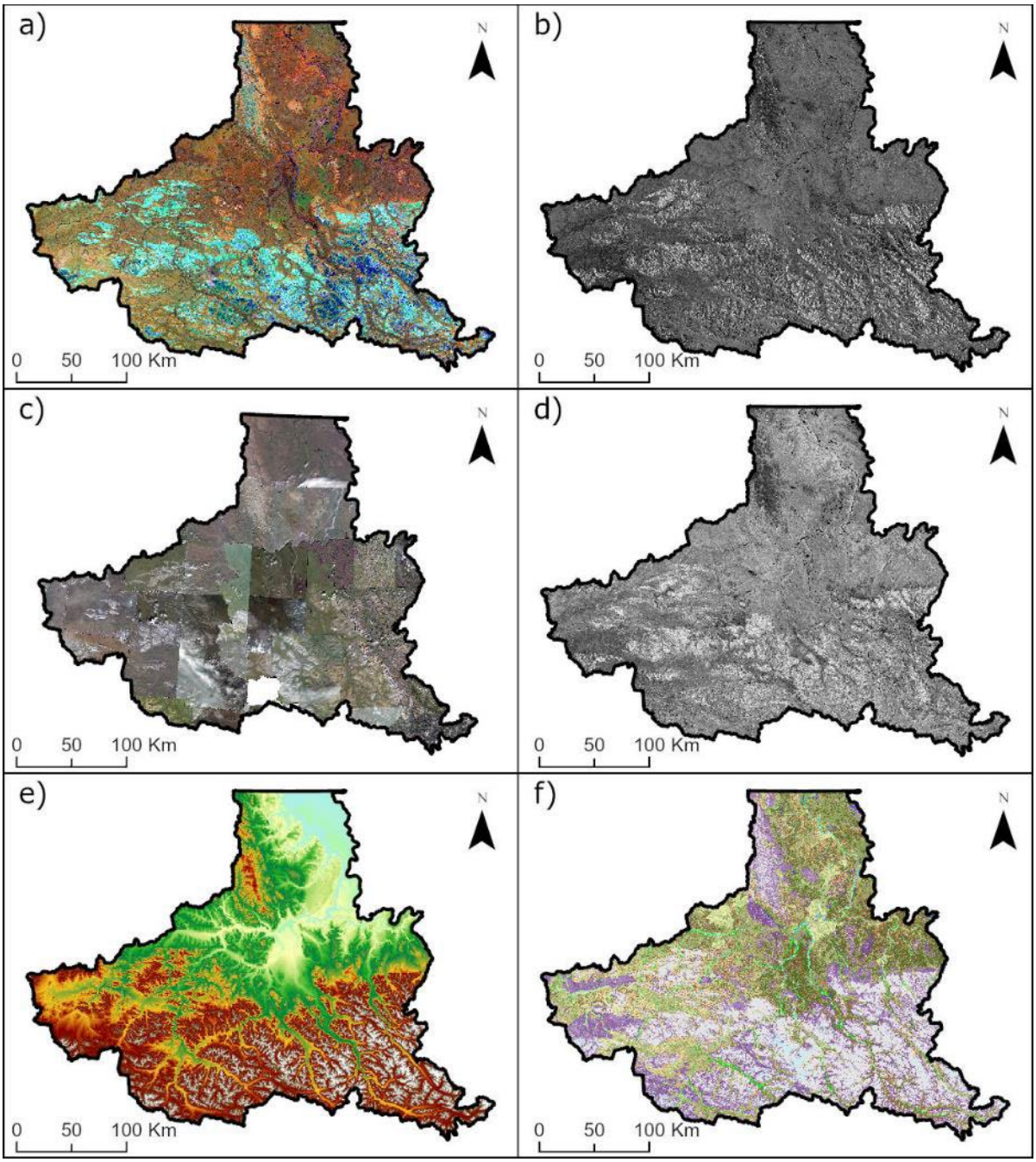

Figure 4: **Satellite imagery used in the wetland classification of the Project Area: a) Sentinel-2 (Red: NIR, Green: SWIR1, Blue: Red), b) Sentinel-1 (VH polarization), c) SPOT 6/7 (8 bit), (d) ALOS PALSAR (HV polarization), e) merged CDEM and ArcticDEM, and f) previous predicting ecological landcover mapping (Meikle & Waterreus 2008)**

2.2.1 SENTINEL-2

Sentinel-2 is an optical (multispectral) satellite operated by the European Space Agency. It has been operating since 2015 with a spatial resolution of 10 to 20 m for the optical spectral bands and a revisit time of five days (Table 2). Due to Sentinel-2's higher spatial (i.e., size of a pixel), temporal (i.e., the time it takes for the satellite to pass over the same location), and spectral (i.e., number of bands the sensor measures) resolutions compared to other open-access satellite data (e.g., Landsat imagery), it is frequently used for landcover classification. The greater spatial and spectral resolutions allow for better discrimination between landcover classes, and the greater temporal resolution increases the chances of capturing cloud-free scenes, facilitating wetland monitoring. In addition, unlike other similar space-based optical sensors, Sentinel-2 includes three red edge bands, which have been shown to have a high potential for wetland discrimination (Ozesmi and Bauer 2002; Adam et al. 2010; Mahdavi et al. 2018; Amani et al. 2018a). Sentinel-2 imagery has previously been used to map wetlands in Yukon (Merchant et al. 2019) and across Canada (Mahdianpari et al. 2021).

Table 2: Sentinel-2 Bands used for Classifying Wetlands in the Project Area and their Central Wavelengths and Resolutions

BAND NAME	CENTRAL WAVELENGTH (µm)	SPATIAL RESOLUTION (m)
Blue	0.490	10
Green	0.560	10
Red	0.665	10
Red Edge 1 (RE1)	0.705	20
Red Edge 2 (RE2)	0.740	20
Red Edge 3 (RE3)	0.783	20
Near Infrared (NIR)	0.842	10
Narrow Near Infrared (NNIR)	0.865	20
Shortwave Infrared 1 (SWIR1)	1.610	20
Shortwave Infrared 2 (SWIR2)	2.190	20

Atmospherically corrected surface reflectance images (i.e., images that have been adjusted for weather and other atmospheric effects; for details see https://sentinel.esa.int/documents/247904/685211/Sentinel-2_User_Handbook) from Sentinel-2 (Level-2A; ee.ImageCollection ("COPERNICUS/S2_SR")) were acquired from Google Earth Engine (GEE). Images with less than 5% cloud cover in July and August between 2018 and 2021 (82 images total, see Appendix A) were selected and a median reducer function (ee.Reducer) was applied to the image stack. This approach was used to create a single composite image containing the median of the pixel values, within the given timeframe, with no/least possible cloud and snow covers. This approach also removed very dark (i.e., shadow) and very bright (e.g., haze, cloud, snow) pixels. Cloud and snow masking is an important pre-processing step in areas such as Yukon due to the predominantly unfavorable weather conditions, particularly in the mountainous regions where cloud and snow cover are frequent. Cloud and snow effectively mask the spectral signatures of the underlying landcover making it challenging or impossible to map correctly. While studies have shown that multi-season optical image is beneficial for landcover mapping due to the ability to discriminate between broadleaf and coniferous species, visual observation of Sentinel-2 images outside July and August revealed the mountainous areas to be impacted by snow cover. As such, multi-temporal images were not utilised

in this project. All Sentinel-2 spectral bands in the final mosaic were resampled to 10 m resolution and projected to WGS 84 UTM Zone 8N.

Multi-season optical image is generally suggested for landcover mapping due to the ability to discriminate between broadleaf and coniferous species. At higher latitudes the growing season, or time of maximum vegetation, is relatively short. Based on visual assessment, images captured in Yukon outside the months of July and August have increasing probability of having snow cover, especially in the mountainous regions. Extensive snow cover in an image can mask the true landcover class attempting to be mapped and can result in poorer map accuracies. Additionally, attempting to produce multi-season mosaics from Sentinel-2 imagery may result in cloudier scenes as the availability of dates for a given mosaic is substantially reduced. Due to these limitations the single mosaic described above sole optical image used in the classification.

2.2.2 SENTINEL-1 AND ALOS PALSAR

The inclusion of SAR imagery has been shown in numerous studies to improve wetland classification (Amani et al. 2017a; Amani et al. 2018b; Amani et al. 2019; Merchant et al. 2019; Adeli et al. 2020; Merchant et al. 2020). SAR sensors measure the backscatter of emitted microwave energy in different polarizations of a single band which influences the ability of the radar signal to penetrate a medium and how it interacts with the surface. For example, C-band has low to moderate penetration and is typically used for landcover mapping and ice and shoreline detection. L-band radar uses a longer wavelength compared to a C-band SAR systems, and thus can increase the ability to penetrate forest cover compared to C-band. As such, L-band sensors are often used for biomass and vegetation mapping. SAR sensors also emit and receive energy in horizontal (denoted by a 'H') or vertical (denoted by a 'V') polarizations. Each polarization carries information about the imaged surface. For example, rough surfaces such as bare soil or water are most sensitive to VV polarization, forest canopies are sensitive to VH and HV, and inundated vegetation is sensitive to HH. Additionally, SAR sensors can capture images through clouds. For this project, imagery from Sentinel-1 (C-band; VV and VH polarizations) and ALOS PALSAR (L-band; HH and HV polarizations) were utilized to combine the benefits of C- and L-band, and multiple polarizations (Table 3).

Table 3: Band, Polarization, and Resolution of Sentinel-1 and ALOS PALSAR Imagery used for Classifying Wetlands in the Study Area

PLATFORM/SENSOR	CENTRAL WAVELENGTH (µm)	POLARIZATION	SPATIAL RESOLUTION (m)
Sentinel-1	5.405 GHz (C-band)	VV, VH	10
ALOS PALSAR	1.270 GHz (L-band)	HH, HV	20

In this project, pre-processed Sentinel-1 imagery (C-band, 5.405 GHz) in VV and VH polarizations were acquired from GEE (ee.ImageCollection ("COPERNICUS/S1_GRD")) from July to August 2020 (41 images total, see Appendix A) in an ascending satellite orbit as Ground Range Detected (GRD) scenes (for pre-processing steps see https://developers.google.com/earth-engine/guides/sentinel1). The pre-processed imagery was mosaicked, and a mean filter (30 m radius) applied to minimize additional remaining noise and the inherent salt and pepper texturing in the data. The Sentinel-1 mosaic, for both VV and VH polarizations, was resampled to 10 m resolution and projected to WGS 84 UTM Zone 8N.

Pre-processed ALOS PALSAR scenes (L-band, 1.27 GHz) were acquired from the Alaska Satellite Facility (ASF) from July and August 2008 to 2010 (76 images total, see Appendix A) in an ascending satellite orbit in Fine Beam Dual (FBD) polarization mode at HH and HV polarizations (for pre-processing steps see https://asf.alaska.edu/data-

sets/sar-data-sets/alos-palsar). The pre-processed imagery was mosaicked, and a 3x3 boxcar filter applied filter to minimize noise and the inherent salt and pepper texturing in the data. Values

were converted to decibels to match the Sentinel-1 imagery. The imagery was mosaicked in ArcGIS and resampled to 10 m spatial resolution and projected to WGS 84 UTM Zone 8N for both the HH and HV polarizations.

ALOS PALSAR imagery was used over the available PALSAR-2 yearly mosaic as the yearly mosaic is compiled using scenes preferentially selected based on their minimal response to soil moisture which makes the imagery less ideal for wetland mapping. The yearly mosaic may also include scenes from the winter months with frozen and/or snow-covered vegetation. It should be noted that the ALOS satellite was decommissioned in early 2011 thus summer imagery after the 2010 season cannot be obtained, and individual scenes, which could be selected for optimal timing, from its successor mission ALOS PALSAR-2 were not available to WSP at the time of this project.

2.2.3 SPOT 6/7

SPOT6/7 satellites are commercial high-resolution satellites (1.5 m spatial resolution) that provide detailed imagery in the red, green, blue, and NIR bands. Near full-coverage of SPOT6/7 imagery was provided for the PWPR as 8-bit RGB, RGB-NIR, or panchromatic scenes. While Amani et al. (2020) found that the inclusion of high-resolution imagery improved the delineation of small landscape features, upon review of the SPOT 6/7 imagery it was determined that some of the images were too cloudy and would decrease classification accuracy. As well, the variability in available bands, lower bit- depths (8 bit vs 16 bit), and incomplete coverage of the study area contributed to the decision to omit the SPOT imagery from segmentation and classification. Instead, the SPOT imagery, in combination with high-resolution Esri World Imagery Basemap available through ArcGIS, was used to supplement the YBIS plot data through visual interpretation by WSP vegetation and wetland specialists.

2.3 TOPOGRAPHIC DATA

Topographical products provide valuable information on elevation, landscape features, and vegetation structure and height, and have been used successfully for wetland mapping (Amani et al. 2020; Millard and Richardson 2013; O'Neil et al. 2018). This is largely because most wetlands form on level to gently sloping terrain, within topographical depressions, or where other conditions allow the water table to reside near the surface (National Wetlands Working Group 1997). However, elevation data on its own does not necessarily assist in separating wetland classes. For example, swamps can occur in both low and high elevation drainages. Elevation derivatives have been shown to capture the spatial patterns that characterize saturated areas, such as the propensity of a site to be wet (O'Neil et al. 2018). Table 4 describes the elevation derivatives used in this study and the rational for their inclusion.

Table 4: Topographical Derivatives used for Classifying Wetlands in the Project Area Derived from the Merged CDEM and ArcticDEM Datasets

DERIVATIVE	RATIONAL
Height Above Nearest Drainage	Related to local draining potential and water table depth which are relevant factors in wetland formation (Nobre et al. 2011)
Aspect	Certain aspects (e.g., steep north vs. south slopes) in the study area have differing vegetation communities (e.g., coniferous vs. sage grassland) (Environment Yukon 2019)
Slope	Wetlands generally occur on level to gently sloping terrain (Environment Yukon 2019; National Wetlands Working Group 1997)
Profile Curvature	Curvature of a slope effects erosional and depositional processes (Moore et al. 1991), and may relate to soil formation and hydrological processes

DERIVATIVE	RATIONAL
Plan Curvature	Curvature of a slope effects flow divergence and convergence (Moore et al. 1991), and may relate to water accumulation

In this project, a combination of the Canadian Digital Elevation Model (CDEM) and ArcticDEM topographic data were used. CDEM for Yukon is available from the GeoYukon portal at a 30 m spatial resolution. The CDEM is derived from existing Canadian Digital Elevation Data which were extracted from the hypsographic and hydrographic elements of the National Topographic Data Base at the scale of 1:50 000, the Geospatial Database, various scaled positional data acquired by the provinces and territories, or remotely sensed imagery (Natural Resources Canada 2013). The CDEM dataset was resampled and merged with the ArcticDEM (2 m spatial resolution resampled to 10 m) which is derived from high resolution optical stereo imagery (Porter et al. 2018). The ArcticDEM covered approximately 93% of the study area and the CDEM was used to fill data gaps (7% of the total merged DEM area). The resultant dataset is a surface model reflecting both bare earth and terrain features at 10 m spatial resolution and projected to WGS 84 UTM Zone 8N. Elevation derivatives, including the aspect, slope, height above nearest drainage (based on the 50k watercourse and waterbody Canvec datasets), as well as profile and plan curvature topographic products were generated in ArcGIS Pro (version 2.9) from the merged DEM for use in the classification.

3 METHODOLOGY

3.1 SEGMENTATION

The multi-resolution segmentation algorithm (Baatz 2000), available in the eCognition software, was used to segment the imagery into meaningful objects. This algorithm is a bottom-up region merging technique that groups neighboring pixels based on the homogeneity criteria. Segmentation was performed using the Sentinel-2 red, green, blue, NIR, and SWIR bands to take advantage of the native 10 m spatial resolution bands (i.e., red, green, blue) for discerning greater detail, and the sensitivity of NIR and SWIR to vegetation and water. Segment size is controlled by the scale parameter, where higher values result in the algorithm producing larger objects. After assessing two different levels, a final scale value of 175 was used to produce then initial wetland versus non-wetland classification, and a value of 100 used for assigning wetland class. The shape (deviation from a compact or smooth shape) and compactness (border length divided by area) parameters were given values of 0.1 and 0.9, respectively, based on trial and error until satisfactory results were achieved. As mentioned in section 2.1, the segmentation was constrained by the training polygons, such that created segments that overlapped the delineated training polygons had the same bounding geometry though could contain several smaller segments.

3.2 SEGMENT STATISTICS

In OBIA, the classification model is trained and applied based on a series of statistics describing each segment (e.g., mean and standard deviation pixel value per segment per spectral band). A common approach to improve model accuracy is by extracting and including additional features, such as band ratios and indices for optical imagery (Amani et al. 2019) and co- (i.e., same sent and received; VV or HH) and cross- (i.e., different sent versus received, VH or HV) polarizations ratios for SAR imagery (Mahdavi et al. 2018). Based on previous studies (Amani et al. 2017a; Amani et al. 2018a,b; Mahdavi et al. 2017; Mahdavi et al. 2018), the features and indices listed in Table 5 were used in the classification as they had the highest potential to discriminate various wetland classes

Table 5: Bands, Indices, Ratios, and Other Features used Included in the Object-Based Random Forest Model

PLATFORM	MODEL INPUT	EQUATION/DESCRIPTION
Sentinel-2	Blue	Segment mean
	Green	Segment mean
	Red	Segment mean
	Red Edge-1	Segment mean
	Red Edge-2	Segment mean
	Red Edge-3	Segment mean
	NIR	Segment mean
	Narrow NIR	Segment mean
	SWIR-1	Segment mean
	SWIR-2	Segment mean

PLATFORM	MODEL INPUT	EQUATION/DESCRIPTION
Sentinel-1	VV	Segment mean
	VH	Segment mean
ALOS PALSAR	HH	Segment mean
	HV	Segment mean
DEM	Elevation	Segment mean
	Height Above Nearest Drainage (HAND)	Segment mean
	Aspect	Segment mean
	Slope	Segment mean
	Profile Curvature	Segment mean
	Plan Curvature	Segment mean
Index	Normalized Differential Vegetation Index (NDVI)	(NIR-Red)/(NIR+Red)
	Normalized Differential Water Index (NDWI)	(Green-NIR)/(Green+NIR)
Ratio	Sentinel-1 Ratio	VH/VV
	ALOS PALSR Ratio	HV/HH
	Textural features	band standard deviation
	Geometry features	object compactness

3.3 OBJECT-BASED RANDOM FOREST CLASSIFICATION

Thresholding techniques were used to mask areas that were likely non-wetlands, such as mountain crests and human development (e.g., roads, buildings), as previous mapping experience showed that the RF algorithm sometimes confused sparse alpine vegetation with the fen and marsh wetland classes. The thresholding was done by assessing the natural breaks in the height above nearest drainage derivative to determine the vertical distance above the nearest mapped drainage in which wetlands were likely not to form based on visual inspection. Anthropogenic disturbances, such as mines, roads, and buildings, were masked using the Brightness statistic in eCognition (the sum of all input layers divided by the number of input layers) and manual methods. Following masking, the RF algorithm was trained using a random selection of two-thirds of the field and interpreted polygons (i.e., training samples) while the remaining one-third were used for the accuracy assessment (i.e., test samples). Objects were assigned a class based on the majority result of all the decision trees created as part of the RF model for that object.

3.4 ACCURACY ASSESSMENT

Accuracy assessments compare the classification with field data to provide information on the overall accuracy and reliability of the map, as well as to understand classification errors (Gopal and Woodcock 1992). Two types of accuracy assessments were conducted for the produced PWRP wetland classification: visual and statistical accuracy assessments.

A simple, but effective type of accuracy assessment is visual inspection. For a visual accuracy assessment, the classification is analysed and interpreted visually using high spatial resolution images (e.g., Esri World Imagery Basemap available in ArcGIS) to see if the mapped classes visually correspond to real features on-the-ground.

Classification accuracy is also statistically assessed through an error matrix using the test samples (see Table 6 as an example). An error matrix is an array with columns representing the assessment data (i.e., samples) and the rows representing the classification data (i.e., mapped class). The numbers within the matrix represent the number of sites assigned to a certain class, where numbers along the main centre diagonal (highlighted cells in Table 6) indicate correctly classified polygons. Numbers in the off-diagonal cells (non-highlighted cells) indicate incorrectly classified polygons and, therefore, potential errors in the map. Overall accuracy (OA) is calculated as the sum of the correctly classified polygons divided by the total number of assessment polygons. Producer's accuracy (PA) is calculated by dividing the total number of polygons correctly classified for a particular class by the total number of assessment polygons for that class and represents polygons that are not classified as the same class as the assessment polygon. User's accuracy (UA) is calculated by dividing the total number of polygons correctly classified for a particular class by the total number of sites classified as that class. This represents polygons that have been assigned a class they do not belong to. It is also important to consider that a polygon may been assigned to the correct class purely by chance. To accommodate for this degree of chance, Cohen's Kappa coefficient is also calculated from the error matrix (Cohen 1960). The Kappa coefficient is a statistic that indicates if the error matrix is significantly different from a random classified result, where values close to 1 indicate a strong agreement between the classified output and the assessment data, and values close to 0 indicate poor agreement.

Table 6: Example Confusion Matrix

		SAMPLES				
		CLASS A	**CLASS B**	**CLASS C**	**ROW TOTAL**	**UA**
MAPPED CLASS	**Class A**	20	1	-	21	20 ÷ 21 = 95%
	Class B	2	10	1	13	10 ÷ 13 = 77%
	Class C	-	1	15	16	15 ÷ 16 = 94%
	Column Total	22	12	16	50	
	PA	20 ÷ 2 = 91%	10 ÷ 12 = 83%	15 ÷ 16 = 94%		OA = 90%

4 RESULTS

4.1 PEEL WATERSHED PLANNING REGION CLASSIFICATION

The produced map identified overall wetland extent across the PWPR, and subsequently mapped five wetland classes: shallow water, marsh, swamp, fen, and bog. The non-wetland areas were broadly classified as expose/disturbed, coniferous forest, broadleaf forest, shrubland, or deep water. Based on the produced map (Figures 5 and 6), wetlands cover approximately 6,000 km^2 (9%) of the PWPR of which fen is the most common, constituting 3,800 km^2 (6%). Marsh covered the least amount of PWPR with 100 km^2 (<1%) mapped in the produced classification. Shallow water coverage was similarly low with 210 km^2 (<1%). Bogs and swamps covered 780 km^2 (1%) and 1,190 km^2 (2%), respectively. Of the non-wetland classes, coniferous forest was the most dominant cover with 21,430 km^2 (%) followed by shrubland with 19,902 km^2 (32%). Table 7 reports the areal coverage of all wetland and non-wetland classes within the PWPR.

Table 7: Area and Percent of the Project Area Occupied by Different Wetland and Non-Wetland Classes

CLASS	AREA (km^2)	% OF PWPR
Wetland		
Shallow water	210	0.31
Marsh	104	0.15
Fen	3,810	5.65
Bog	783	1.16
Swamp	1,189	1.76
Total Wetland	*6,097*	*9.05*
Non-wetland		
Deep water	678	1.01
Exposed/disturbed	18,262	27.10
Coniferous forest	21,430	31.8
Broadleaf forest	1,020	1.51
Shrubland	19,902	29.53
Total Non-wetland	*61,293*	*90.95*
Total Area (Wetland, Non-Wetland)	**67,390**	**100.00**

The majority of wetlands were mapped in the northern portion of the PWPR, particularly in the Peel Plateau and Fort MacPherson Plain ecoregions, with few wetlands occurring in the Mackenzie Mountains and British-Richardson Mountains ecoregions. Large wetland complexes generally occurred on gently sloping or level terrain in large valleys or plains, whereas small, isolated wetlands were found in valley bottoms within the mountainous southern areas.

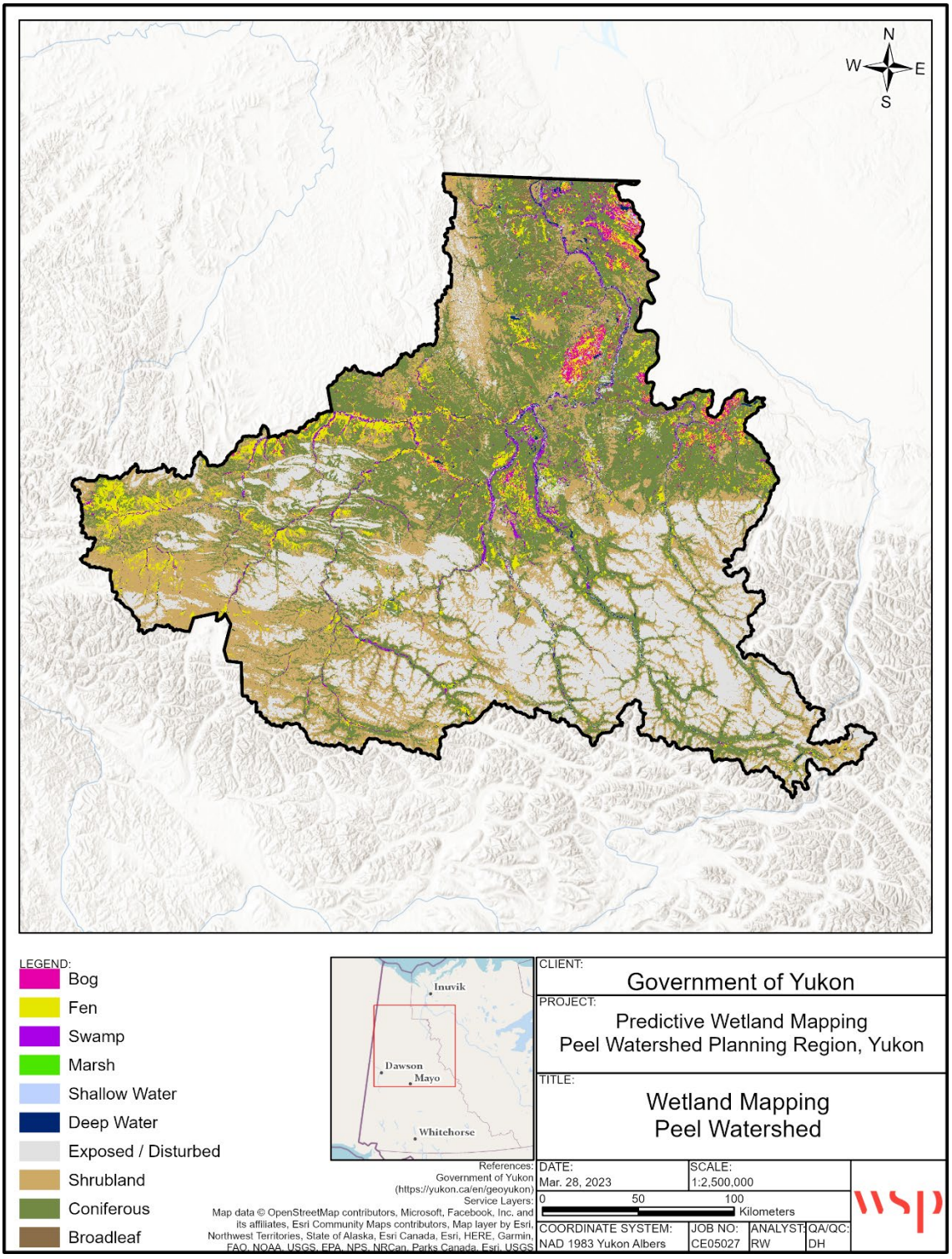

Figure 5: Predictive wetland classification for the Peel Watershed Planning Region

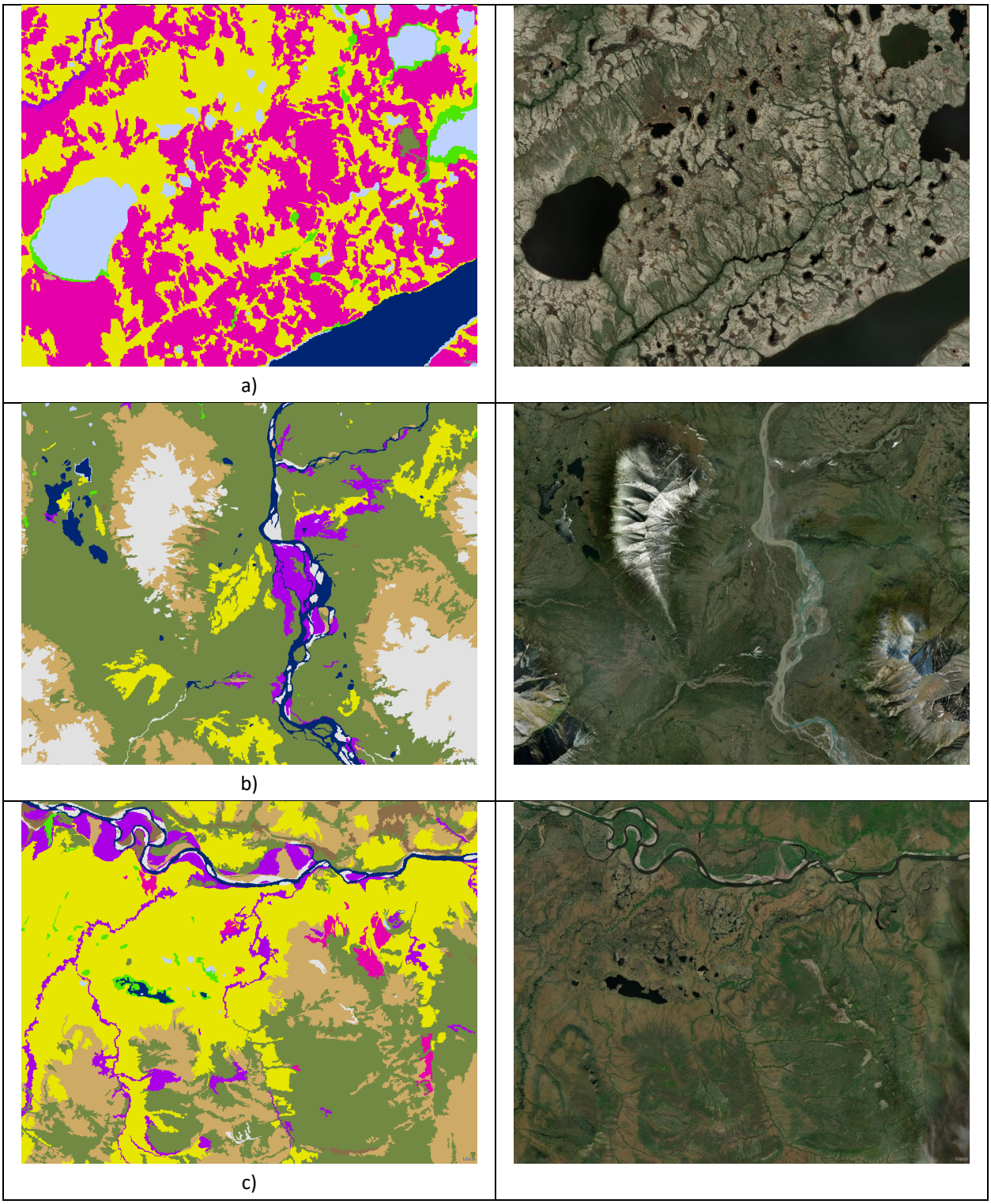

Figure 6: **Classification examples at a 1:50,000 scale (left) compared to the satellite imagery (right), where bogs are shown in pink, fens in yellow, swamps in purple, marshes in bright green, and shallow water in light blue. All other colours represent non-wetlands**

4.2 CLASSIFICATION ASSESSMENT

The wetland classification was visually assessed by WSP, Government of Yukon, and First Nation of Na-Cho Nyak Dun, and comments were reviewed and incorporated into the final product. Upon final visual inspection, most of the classified areas appeared to be visually realistic, conform to landscape patterns, and correspond with features visible in the Esri Basemap and SPOT 6/7 imagery. Although there was some confusion between some of the wetland and non-wetland classes, the accuracy levels that are obtained in this study are high considering the complexity of wetlands and the PWPR.

Furthermore, the accuracy of the produced classification was statistically assessed using a confusion matrix obtained based on the classification, and combined field and interpreted sites set aside for product validation. Table 8 provides the overall classification accuracy (OA), Table 9 provides the classification accuracy for each respective wetland class (PA and UA), and Table 10 provides the amount of misclassification (confusion) between various wetland class pairs on a per pixel basis. The pixel-based accuracy assessment indicates the likelihood that a randomly selected pixel was classified correctly. Wetland extent across the PWPR was mapped with an accuracy of 92.46% and the five major wetland classes were mapped with an accuracy of 79.85%. Of the wetland classes, shallow water obtained the highest PA (89.88%), indicating that most of the assessment data was classified correctly. Bog and fen achieved high to moderately high PA at 85.39% and 79.44%, respectively. Swamp and marsh obtained the lowest PA with 69.92% and 68.81%, respectively, as well as the lowest UA (67.96% and 56.82%), indicating that there were several assessment samples of other classes which were wrongly classified as either swamp or marsh. In central Yukon, marshes are less common on the landscape in comparison to peatlands, and where they do occur tend to be limited to thin bands along shorelines. The 10 m spatial resolution Sentinel-2 imagery used in this project may not be able to properly capture these features, which could be addressed through the inclusion of high-resolution imagery such as SPOT. Marsh vegetation can also be similar to the characteristic species found in graminoid fens (e.g., sedges). Swamps tend to be relatively common in central to northern Yukon; however, they are often confused with fens and non-wetlands due to overlapping characteristics. For example, these classes all have coniferous treed or shrubby forms and overlay organic soils (Environment Yukon 2019). Additionally, these three wetland classes often transition between each other resulting in sites that have characteristics of multiple classes limiting the ability to separate these classes based solely on spectral signatures.

Table 8: The Overall, Producer, and User Classification Accuracies for Deep Water, Wetlands, and Uplands on a Per Pixel Basis

OVERALL ACCURACY: 92.46%	KAPPA COEFFICIENT: 0.85	USER ACCURACY (%)
CLASS	PRODUCER ACCURACY (%)	
Deep water	98.94	92.10
Wetland	86.57	90.83
Upland	94.89	93.27

Table 9: The Overall, Producer, and User Classification Accuracies of the Wetland Classes on a Per Pixel Basis

OVERALL ACCURACY: 79.85%	KAPPA COEFFICIENT: 0.64	USER ACCURACY (%)
CLASS	PRODUCER ACCURACY (%)	
Bog	85.39	99.04
Fen	79.44	94.79
Swamp	69.92	67.97
Marsh	68.81	56.82
Shallow Water	89.88	94.67

Table 10: Confusion Matrix For the Wetland Classes Calculated on a Per Pixel Basis

MAPPED CLASS	REFERENCE SAMPLES (PERCENT OF PIXELS)					
		BOG	FEN	SWAMP	MARSH	SHALLOW WATER
	Non-wetland	3.14	16.02	21	1.36	8.61
	Bog	85.39	0.23	0	0.05	0
	Fen	11.1	79.44	3.83	26.8	0.76
	Swamp	0	3.41	69.92	0.15	0
	Marsh	0.35	0.89	5.26	68.81	0.76
	Shallow Water	0.02	0.01	0	2.83	89.88

An object-based accuracy assessment was additionally produced at the polygon level and is presented along with the class PA and UA in Appendix B. The object-based accuracy assessment indicates how likely a wetland or non-wetland polygon of interest was classified correctly. Based on the confusion matrix produced from the classified objects, an OA of 82.98% was achieved with an average PA for the wetland classes of 71.94%.

5 DISCUSSION

5.1 TRAINING DATA LIMITATIONS

Although the optimum number of field samples for training machine learning algorithms and accuracy assessment is dependent on several factors, including the number and distribution of classes (McNairn et al. 2009), it has been extensively discussed that generally increasing the number of training data results in more reliable classifications with higher accuracies (Amani et al. 2017b). In total, 1,138 polygons (529 YBIS field plots and 608 satellite interpreted sites) were delineated for training and assessment data. The YBIS plots were skewed to non-wetland areas where 327 plots represented upland classes (i.e., coniferous, broadleaf, shrubland, exposed/disturbed) and 187 represented wetland classes. The interpreted polygons were more evenly split, though biased towards wetlands, with 355 wetland polygons and 253 non-wetland polygons. Exposed/disturbed, coniferous forest, shrubland, fen, and bog were well sampled in the combined training and assessment datasets, whereas shallow water, marsh, and broadleaf forest has lower sample density. Similarly, the swamp class was low to moderately sampled compared to other classes. The low number of samples, along with the relative rarity of marsh with the PWPR, and spectral similarity of marsh, shallow water, and swamp to other classes may have affected RF model accuracy and explain the lower PA and UA for these classes. The lower PA for exposed/disturbed was likely due to the over classification of shrubland to include very sparsely vegetated alpine or riparian sites.

Since the YBIS data was collected previous to this project, additional field data could not be captured to create a more representative dataset. The satellite interpreted polygons were delineated to supplement gaps in the YBIS data and increase the number of training sites for the PWPR. However, shallow water can be a difficult class to identify in satellite imagery due to the limitations on confidently determining water depth with optical or SAR imagery, and its spectral similarity to other classes (e.g., deep water). Based on previous experience mapping wetlands in the Yukon, it was observed that marshes tend to be relatively uncommon and small. As a result, the marsh class tends to have fewer samples than other more spatially extensive classes, such as fens. In the Yukon, swamps can also be difficult to identify from satellite imagery as they share similar vegetation to uplands and peatlands (e.g., wooded coniferous forms) whereby, they can only be defined by hydric soil properties (e.g., gleying, peat depth) (Environment Yukon, 2019), which are only discernible from the ground.

As previously discussed, only the southern and northern regions of the PWPR were extensively sampled with few YBIS plots representing the central and western areas. In particular, the western and north-western regions (i.e., North Ogilvie Mountains, Eagle Plains, British-Richardson Mountains) host distinctly different landscapes than those observed in the Mackenzie Mountains and Peel Plateau. As a result, the wetland training data does not perfectly represent these regions; however, interpreting training data from satellite imagery alone proves challenging due to low species biodiversity resulting in high spectral similarity between classes (e.g., wet tundra versus peatland). Furthermore, the field data in this project were collected during different years varying from 1975 to 2020. This temporal disparity across field data collections as well as between data collection and image acquisition could also cause uncertainty in the classification. This temporal difference is most important as it relates to YBIS plots as some plots were surveyed prior to the occurrence of a forest fire which alters the spectral signature and possibly even the landcover class. Additionally, plots sampled after a fire may have undergone significant landscape change as the result of vegetation regrowth and succession, or loss of permafrost or organic material. Thus, it is suggested additional field data be collected in future wetland classifications of the PWPR.

5.2 IMAGERY LIMITATIONS

Amani et al. (2020) found that the inclusion of high-resolution imagery improved the delineation of small landscape features. Government of Yukon has near full coverage of SPOT 6/7 imagery for the PWPR; however, this imagery was unable to be incorporated in the segmentation and classification due to technical and logistical limitations. The available SPOT 6/7 imagery had significant cloud cover in some areas, as well as variable image date, and non-optimal timing (i.e., imagery not captured during peak growing season). Due to the technical challenges in incorporating the SPOT 6/7 imagery and project timelines, it was decided to omit the imagery from segmentation and classification and reserve it for site interpretation and visual accuracy assessment of the final product. It is suggested to refine these images and resolve these technical limitations to use them in future wetland classifications in Yukon.

5.3 LIMITATIONS FOR WETLAND MAPPING IN YUKON

The results of this study show that regardless of the satellite data being used, wetlands due to their complexity, can hinder the achievement of higher classification accuracies compared to other land covers. For instance, wetland classes have several spectral similarities due to their biological and hydrological characteristics (Mitsch and Gosselink 2000; Amani et al. 2018a). This is especially apparent when mapping at higher latitudes where a decrease in biodiversity results in smaller spectral differences between classes (Figure 7). This can also be compounded by previous forest fires altering or masking the spectral response of a particular landcover. Considering these facts and comparing the results with other wetland studies, the produced overall wetland classification accuracy of 79.85% in this project is very good. However, some confusion still existed between wetland classes most notably between fens, swamps, and bogs, as well as between marshes and shallow water (<2 m). In both cases this confusion is likely the result of overlapping ecosite characteristics, such as species and wetness. For example, wooded coniferous fens and swamps can host similar species and differ based on the specific characteristics of the soil and vegetation (i.e., size), which are not readily observed in satellite imagery. While the combination of optical, SAR, and topographical data improved the separability between similar classes, wetlands themselves are highly variable and transitional ecosystems making them difficult to classify both on the ground and through remote sensing methods.

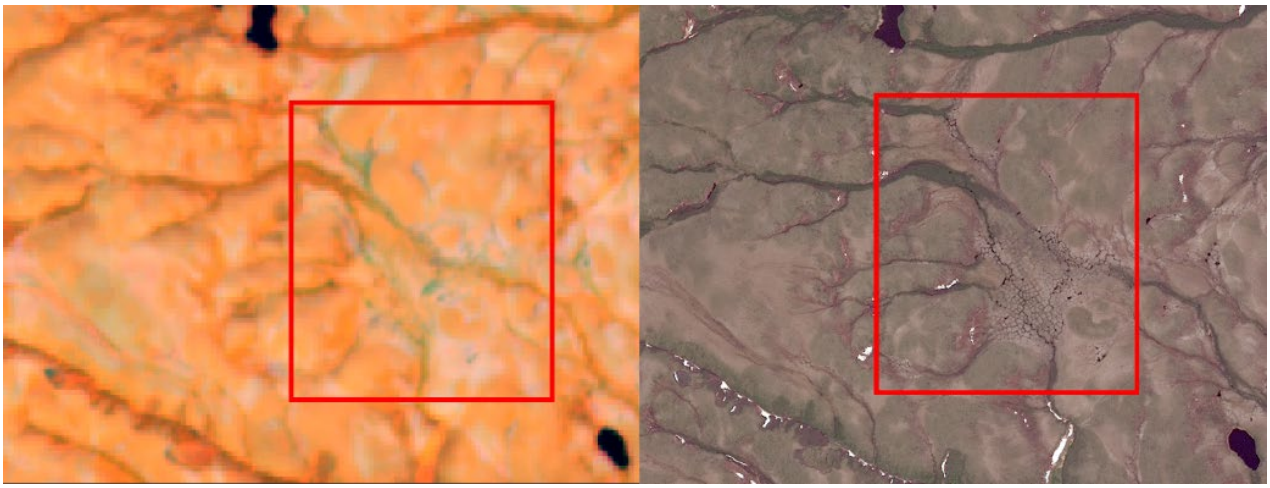

Figure 7: Example of a high latitude wetland in Sentinel-2 (left) and Spot 6/7 (right) imagery. The spectral signatures of the wetland and surrounding shrub tundra are similar making it difficult for a model to sperate the features

5.4 RECOMMENDATIONS

The PWPR is a 67,431 km^2 area in northern Yukon characterized by mountains in the south and extensive wetland complexes in the north. The size and landscape variability observed in the watershed provided a number of logistical challenges during the mapping process that should be considered in future mapping projects. In an object-based approach the user determines the size of the objects to be created. Smaller objects can capture a greater number of details in the landscape; however, comes at the cost of increased processing time as the model needs to sample and classify over a greater number of objects. Over a large project area, such as the PWPR, reducing object size can substantially increase computing time and a trade-off needs to be made between detail and time. The object size selected in this project was small enough to capture key landscape features (e.g., raised bogs surrounded by fen) but did not always capture small features such as shoreline marshes and drainage swamps, or the small variations between classes within a wetland complex. In order to utilize a small segmentation for the PWPR or other large project areas it is recommended that the PWPR be sub-divided or additional time be allotted to account for the longer processing times. Along with segmentation scale, including higher resolution imagery (e.g., SPOT 6/7, high-resolution DEM) also significantly increases processing time for both the pre-processing and classification which may limit their use in large-scale mapping efforts. A subsequent study is recommended to assess the utility of commonly used datasets for wetland classification (e.g., optical, SAR and topographic imagery) to identify the most important for inclusion and reduce computational requirements with minimal decreases to accuracy.

On review of the draft classification, it was noted that fens in the north-west of the PWPR were not identified as wetlands by the RF model. As previously mentioned, this was likely in part due to the majority of the training data being located in the eastern portions of the PWPR. Additional training sites were added to improve the classification; however, the model continued to have trouble identifying similar sites. Thus, it is recommended that the PWPR, and other large projects should be sub-divided into areas of similar landscape characteristics, such as by ecoregion. The training data should additionally be collected for each sub-area to ensure the sites are representative of the classes found in each particular region. This, however, may be challenging when some areas lack previously collected data or are generally inaccessible for collecting large amounts of ground data. Future field

campaigns to collect addition survey sites should be focused on areas where it is difficult to determine landcover solely from satellite imagery, for example the North Ogilvie and British-Richardson Mountains ecoregions.

Lastly, various model iterations were run using various subsets of data and applied over isolated areas to improve the classification where known confusion was occurring. The results of this process suggested that further improvements in accuracy may not be achieved by the RF model alone. Previous mapping experience in Yukon and Northwest Territories supports this assessment, whereby higher accuracies were obtained after completing extensive manual refinement. The decrease in species diversity and complex systems influenced by permafrost may be the reason for this, though regardless further research into novel remote sensing techniques, such as deep learning, is likely required for northern wetland mapping in Canada.

6 CONCLUSION

WSP developed an object-based RF model that identified wetlands (i.e., shallow water, marsh, fen, bog, swamp) and non-wetlands (i.e., deep water, coniferous forest, broadleaf forest, shrubland, exposed/disturbed) within the Peel Watershed Planning Region. According to the results, about 9% of the total area within the study area is comprised of wetlands, in comparison to previous estimates of 6% (Yukon Ecoregions Working Group 2004, p. 75-156) and 0.8% (Meikle and Waterreus 2008). Large wetland complexes were identified in the northern portion of the watershed, particularly in the Peel Plateau and Fort MacPherson Plain ecoregions, with few wetlands occurring in the Mackenzie Mountains and British-Richardson Mountains ecoregions. Of the wetland classes, fens were the most common by area, followed by swamps, bogs, shallow water, and finally marshes. The overall wetland classification accuracy was 79.85%, with bogs and shallow water achieving the highest producer's and user's accuracies, fen reporting modest accuracies, and swamp and marsh receiving the lowest accuracies. These results show that the approach used in this project has a high potential for wetland classification in future studies and will assist in management decisions related to land use planning and management of the Peel Watershed Planning Region.

7 REFERENCES

Adam, E., O. Mutanga and D. Rugege. 2010. *Multispectral and Hyperspectral Remote Sensing for Identification and Mapping of Wetland Vegetation: A Review*. Wetlands Ecology and Management, 18(3), 281-296.

Adeli, S., B. Salehi, M. Mahdianpari, L.J. Quackenbush, B. Brisco, H. Tamiminia, and S. Shaw. 2020. *Wetland Monitoring using SAR Data: A Meta-analysis and Comprehensive Review*. Remote Sensing, 12(14), 2190.

Amani, M., B. Salehi, S. Mahdavi, and B. Brisco. 2018a. *Spectral Analysis of Wetlands using Multi-source Optical Satellite Imagery*. ISPRS journal of photogrammetry and remote sensing, 144, 119-136.

Amani, M., B. Salehi, S. Mahdavi, B. Brisco, and M. Shehata. 2018b. *A Multiple Classifier System to Improve Mapping Complex Land Covers: A Case Study of Wetland Classification using SAR Data in Newfoundland, Canada*. International Journal of Remote Sensing, 1-14.

Amani, M., B. Salehi, S. Mahdavi, and B. Brisco. 2019. *Separability Analysis of Wetlands in Canada using Multi-source SAR Data*. GIScience & Remote Sensing, 56(8), 1233-1260.

Amani, M., B. Salehi, S. Mahdavi, J. Granger, and B. Brisco. 2017a. *Wetland Classification in Newfoundland and Labrador using Multi-source SAR and Optical Data Integration*. GIScience & Remote Sensing, 54(6), 779-796.

Amani, M., B. Salehi, S. Mahdavi, J.E. Granger, B. Brisco, and A. Hanson. 2017b. *Wetland Classification using Multi-source and Multi-temporal Optical Remote Sensing Data in Newfoundland and Labrador, Canada*. Canadian Journal of Remote Sensing, 43(4), 360-373.

Amani, M., S. Mahdavi and O. Berard. 2020. *Supervised Wetland Classification using High Spatial Resolution Optical, SAR, and LiDAR Imagery*. Journal of Applied Remote Sensing, 14(2), 024502.

Baatz, M. 2000. *Multi Resolution Segmentation: An Optimum Approach for High Quality Multi Scale Image Segmentation*. In Beutragezum AGIT-Symposium. Salzburg, Heidelberg, 2000 (pp. 12-23).

Blaschke, T. 2010. *Object Based Image Analysis for Remote Sensing*. ISPRS journal of photogrammetry and remote sensing, 65(1), 2-16.

Breiman, L. 2001. *Random Forests*. Machine learning, 45(1), 5-32.

Cohen, J. 1960. *A Coefficient of Agreement for Nominal Scales*. Educational and Psychological Measurement, 20(1), 37-46.

Corcoran, J., J. Knight, K. Pelletier, L. Rampi, and Y. Wang. 2015. *The Effects of Point or Polygon-based Training Datamon Random Forest Classification Accuracy of Wetlands*. Remote Sensing, 7(4), 4002–4025.

CryoGeographic Consulting. 2018. *Mapping and Classifying Wetlands in the Indian River Alley, Yukon*. CryoGeographic Consulting and Palmer Environmental Consulting Group Inc., Whitehorse, YT, Canada.

Ecological and Landscape Classification of Ecoregions Technical Working Group. 2014. *Ecoregions of Yukon: Revisions to the Yukon portion of the National Ecological Framework*. Department of Environment, Policy, Planning & Aboriginal Relations Branch, Government of Yukon, Whitehorse, Yukon.

Environment Yukon. 2016. *Yukon Ecological and Landscape Classification and Mapping Guidelines (Version 1.0).* Department of Environment, Government of Yukon, Whitehorse, YT, Canada.

Environment Yukon. 2019. *Klondike Plateau Boreal Low Subzone (BOLkp): A Field Guide to Ecosite Identification*. Department of Environment, Government of Yukon, Whitehorse, YT, Canada.

Gopal, S. and C. Woodcock. 1992. *Accuracy Assessment of the Stanislaus Vegetation Map using Fuzzy Sets*. Remote Sensing and Natural Resource Management: Proceedings of the Fourth Forest Service Remote Sensing Applications Conference, 378-394. American Society for Photogrammetry and Remote Sensing, USA.

Mahdavi, S., B. Salehi, J. Granger, M. Amani, B. Brisco, and W. Huang. 2018. *Remote Sensing for Wetland Classification: A Comprehensive Review*. GIScience & remote sensing, 55(5), 623-658.

Mahdavi, S., B. Salehi, M. Amani, J.E. Granger, B. Brisco, W. Huang, and A. Hanson. 2017. *Object-based Classification of Wetlands in Newfoundland and Labrador using Multi-temporal PolSAR Data*. Canadian Journal of Remote Sensing, 43(5), 432-450.

Mahdianpari, M., B. Brisco, J.E. Granger., F. Mohammadimanesh, B. Salehi, S. Homayouni, and L. Bourgeau-Chavez. 2021. *The Third Generation of Pan-Canadian Wetland Map at 10 m Resolution using Multisource Earth Observation Data on Cloud Computing Platform*. IEEE Journal of Selected Topics in Applied Earth Observations and Remote Sensing 14 (2021): 8789-8803.

McNairn, H., C. Champagne, J. Shang, D. Holmstrom, and G. Reichert. 2009. *Integration of Optical and Synthetic Aperture Radar (SAR) Imagery for Delivering Operational Annual Crop Inventories*. ISPRS Journal of Photogrammetry and Remote Sensing, 64(5), 434-449.

Meikle, J.C. and M.B. Waterreus. 2008. *Ecosystems of the Peel Watershed: A Predictive Approach to Regional Ecosystem Mapping*. Yukon Fish and Wildlife Branch Report TR-08-01. 66 pp.

Merchant, M.A., C. Hass, J. Schroder, R.K. Warren, and R. Edwards. 2020. *High-latitude Wetland Mapping using Multidate and Multisensor Earth Observation Data: A Case Study in the Northwest Territories*. Journal of Applied Remote Sensing 14, no. 3 (2020): 034511.

Merchant, M.A., R.K. Warren, R. Edwards, and J.K. Kenyon. 2019. *An Object-Based Assessment of Multi Wavelength SAR, Optical Imagery and Topographical Datasets for Operational Wetland Mapping in Boreal Yukon, Canada*. Canadian Journal of Remote Sensing.

Millard, K. and M. Richardson. 2013. *Wetland Mapping with LiDAR Derivatives*, SAR Polarimetric Decompositions, and LiDAR–SAR Fusion using a Random Forest Classifier Canadian Journal of Remote Sensing, 39(4), 290-307.

Mitsch, W.J. and J.G. Gosselink. 2000. *Wetlands*, third ed. Wiley, New York.

Moore, I.D., R.B. Grayson, and A.R. Ladson. 1991. *Digital Terrain Modelling: A Review of Hydrological, Geomorphological, and Biological Applications Hydrological Processes*, 5(1), 3-30.

National Wetlands Working Group. 1997. *The Canadian Wetland Classification System*. National Wetland Working Group, University of Waterloo, Wetlands Research Centre, Waterloo, ON, Canada.

Natural Resources Canada. 2013. *Canadian Digital Elevation Model: Product Specifications – Edition 1.1*. Government of Canada, Ottawa, ON, Canada.

Nobre, A.D., L.A. Cuartas, M. Hodnett, C.D. Rennó, G. Rodrigues, A. Silveira, and S. Saleska. 2011. *Height Above the Nearest Drainage–a hydrologically Relevant New Terrain Model*. Journal of Hydrology, 404(1-2), 13-29.

O'Neil, G.L., J.L. Goodall and L.T. Watson. 2018. *Evaluating the Potential for Site-specific Modification of LiDAR DEM Derivatives to Improve Environmental Planning-scale Wetland Identification using Random Forest Classification*. Journal of Hydrology, 559, 192-208.

Ozesmi, S.L. and M.E. Bauer. 2002. *Satellite Remote Sensing of Wetlands*. Wetlands Ecology and Management, 10(5), 381-402.

Porter, C., P. Morin, I. Howat, M-J Noh, B. Bates, K. Peterman, S. Keesey, M. Schlenk, J. Gardiner, K. Tomko, M. Willis, C. Kelleher, M. Cloutier, E. Husby, S. Foga, H. Nakamura, M. Platson, M. Wethington Jr, C. Williamson, G. Bauer, J. Enos, G. Arnold, W. Kramer, P. Becker, A. Doshi, C. D'Souza, P. Cummens, F. Laurier, and M. Bojesen. 2018. ArcticDEM. [Data set]. Polar Geospatial Center and Harvard Dataverse.

Soil Classification Working Group. 1998. *The Canadian System of Soil Classification*, 3rd ed. Publication 1646. Research Branch. Agriculture and Agri-Food Canada. Ottawa, ON.

White, M.P., C.A.S. Smith, D. Kroetsch and K.M. McKenna. 1992. *Soil Landscapes of Yukon*. Agriculture and Agri-Food Canada (database and map at 1:1,000,000 scale).

Yukon Ecoregions Working Group. 2004. *Yukon Plateau-North*. In: Ecoregions of the Yukon Territory: Biophysical properties of Yukon landscapes, C.A.S. Smith, J.C. Meikle and C.F. Roots (eds.), Agriculture and Agri-Food Canada, PARC Technical Bulletin No. 04-01, Summerland, British Columbia, p. 63-72.

Yukon Government. 2022. *Yukon Biophysical Inventory System – Site, Soil and Vegetation*. https://apps.gov.yk.ca/yeis-biophys.

Appendix A

Imagery Data Sources

SENTINEL-2 IMAGES

Sentinel-2 Level 2A products are presented in granules, also called tiles, 110 km^2 by 110 km^2 ortho-images projected in WGS84 UTM. Each tile overlaps its neighbouring tiles considerably. The tile grid can be downloaded in KML format at:
https://sentinels.copernicus.eu/documents/247904/1955685/S2A_OPER_GIP_TILPAR_MPC__20151209T095117_V20150622T000000_21000101T000000_B00.kml

Table A1: List of Sentinel-2 Images used to Create the Median Mosaic for the Object-based Random Forest Classification

PLATFORM	SENSING DATE	TILE	ORBIT	CLOUDY PIXEL PERCENTAGE	CLOUD SHADOW PERCENTAGE	SNOW/ICE PERCENTAGE
Sentinel-2A	2019-07-12	08WPS	Ascending	3.62	0.66	0.33
Sentinel-2A	2019-07-12	08WPT	Ascending	4.03	0.81	0.04
Sentinel-2A	2019-07-12	08WPU	Ascending	3.84	1.61	0.00
Sentinel-2A	2019-07-15	08WNS	Ascending	3.66	1.86	0.02
Sentinel-2A	2019-07-22	08WNV	Ascending	0.91	1.19	0.00
Sentinel-2B	2019-07-23	07WFP	Ascending	0.96	0.00	0.00
Sentinel-2B	2019-07-23	08WMT	Ascending	4.40	3.40	0.03
Sentinel-2B	2019-07-23	08WNV	Ascending	4.41	0.31	0.00
Sentinel-2B	2019-07-27	08WMT	Descending	1.55	0.40	0.00
Sentinel-2B	2019-07-27	08WNU	Descending	1.94	0.22	0.00
Sentinel-2B	2019-07-27	08WNV	Descending	3.49	0.47	0.09
Sentinel-2B	2019-07-02	07WFP	Descending	1.01	0.45	0.00
Sentinel-2B	2019-07-27	08WMU	Descending	0.39	0.00	0.00
Sentinel-2A	2019-08-05	08WNT	Descending	4.32	4.05	0.01
Sentinel-2A	2019-08-05	08WNU	Descending	0.55	0.10	0.00
Sentinel-2A	2019-08-05	08WPU	Descending	0.58	0.54	0.00
Sentinel-2A	2019-08-25	08WNU	Descending	0.18	0.34	2.24
Sentinel-2A	2019-08-25	08WPU	Descending	1.89	1.45	2.78
Sentinel-2B	2020-07-31	07WEM	Ascending	1.70	0.10	0.03
Sentinel-2B	2020-07-31	07WEN	Ascending	0.07	0.01	0.01
Sentinel-2B	2020-07-31	07WFM	Ascending	2.40	0.32	0.03
Sentinel-2B	2020-07-31	07WFP	Ascending	1.84	0.65	0.00
Sentinel-2B	2020-07-31	08WMU	Ascending	1.30	0.92	0.00
Sentinel-2B	2020-07-31	08WMV	Ascending	3.35	2.20	0.02
Sentinel-2B	2020-07-31	08WNT	Ascending	0.72	0.75	0.27
Sentinel-2B	2020-07-31	08WNU	Ascending	0.39	0.65	0.00
Sentinel-2B	2020-07-31	08WNV	Ascending	0.00	0.00	0.00
Sentinel-2B	2020-07-31	08WPS	Ascending	0.77	1.06	0.52
Sentinel-2B	2020-07-31	08WPT	Ascending	0.40	0.41	0.16
Sentinel-2B	2020-07-31	08WPU	Ascending	0.02	0.03	0.00

PLATFORM	SENSING DATE	TILE	ORBIT	CLOUDY PIXEL PERCENTAGE	CLOUD SHADOW PERCENTAGE	SNOW/ICE PERCENTAGE
Sentinel-2A	2020-08-02	08WMU	Ascending	2.77	0.19	0.00
Sentinel-2B	2020-08-06	08WMT	Descending	3.75	2.84	0.00
Sentinel-2A	2020-08-22	08WNV	Ascending	4.21	0.35	0.00
Sentinel-2A	2021-07-01	07WEM	Descending	1.26	0.20	0.18
Sentinel-2A	2021-07-01	07WEN	Descending	0.60	0.35	0.01
Sentinel-2A	2021-07-01	07WFM	Descending	0.69	0.70	0.26
Sentinel-2A	2021-07-01	07WFN	Descending	4.48	0.23	0.03
Sentinel-2B	2021-07-02	07WEM	Ascending	3.85	1.82	0.09
Sentinel-2B	2021-07-02	07WFM	Ascending	2.08	0.81	0.31
Sentinel-2B	2021-07-02	07WFN	Ascending	3.90	1.36	0.01
Sentinel-2B	2021-07-02	07WFP	Ascending	0.07	0.00	0.00
Sentinel-2B	2021-07-02	08WMT	Ascending	0.10	0.05	0.00
Sentinel-2B	2021-07-12	07WEN	Ascending	3.19	2.19	0.02
Sentinel-2B	2021-07-12	07WFN	Ascending	2.40	1.67	0.01
Sentinel-2B	2021-07-12	07WFP	Ascending	2.24	2.24	0.00
Sentinel-2B	2021-07-12	08WMT	Ascending	2.94	3.23	0.00
Sentinel-2B	2021-07-12	08WMU	Ascending	2.11	2.31	0.00
Sentinel-2B	2021-07-12	08WMV	Ascending	4.04	2.26	0.08
Sentinel-2A	2021-07-17	08WPS	Ascending	1.18	1.80	1.71
Sentinel-2A	2021-07-17	08WMT	Ascending	0.67	0.97	0.00
Sentinel-2A	2021-07-17	08WMU	Ascending	3.33	3.80	0.03
Sentinel-2A	2021-07-17	08WMV	Ascending	2.90	1.98	0.01
Sentinel-2A	2021-07-17	08WNV	Ascending	0.64	0.53	0.01
Sentinel-2B	2021-07-20	08WNU	Ascending	1.87	0.00	0.00
Sentinel-2B	2021-07-20	08WPU	Ascending	2.59	0.00	0.00
Sentinel-2A	2021-07-24	07WFM	Ascending	1.80	1.67	0.01
Sentinel-2A	2021-07-24	07WFN	Ascending	0.75	0.73	0.02
Sentinel-2A	2021-07-24	08WMT	Ascending	1.02	0.52	0.02
Sentinel-2A	2021-07-24	08WMU	Ascending	0.41	0.00	0.00
Sentinel-2A	2021-07-24	08WNT	Ascending	1.46	0.03	0.00
Sentinel-2A	2021-07-31	07WEM	Ascending	1.98	2.04	0.01
Sentinel-2A	2021-07-31	07WEN	Ascending	0.00	0.00	0.00
Sentinel-2A	2021-07-31	08WNS	Ascending	2.35	2.14	0.06
Sentinel-2A	2021-07-31	08WNT	Ascending	4.20	4.13	0.02
Sentinel-2A	2021-07-31	08WPS	Ascending	0.29	0.47	0.18
Sentinel-2A	2021-07-31	08WPU	Ascending	2.07	0.50	0.00
Sentinel-2A	2021-08-01	08WPS	Descending	0.72	1.92	0.62
Sentinel-2B	2021-08-01	07WEM	Ascending	0.99	0.01	0.00
Sentinel-2B	2021-08-01	07WFM	Ascending	0.06	0.06	0.01

PLATFORM	SENSING DATE	TILE	ORBIT	CLOUDY PIXEL PERCENTAGE	CLOUD SHADOW PERCENTAGE	SNOW/ICE PERCENTAGE
Sentinel-2B	2021-08-02	08WMS	Ascending	2.90	0.17	0.03
Sentinel-2B	2021-08-02	08WMT	Ascending	0.18	0.02	0.00
Sentinel-2B	2021-08-02	08WNT	Ascending	0.06	0.07	0.02
Sentinel-2B	2021-08-02	08WPT	Ascending	0.04	0.09	0.01
Sentinel-2B	2021-08-05	07WFP	Ascending	2.99	0.00	0.00
Sentinel-2B	2021-08-05	08WMU	Ascending	2.90	0.01	0.00
Sentinel-2B	2021-08-05	08WMV	Ascending	0.02	0.02	0.00
Sentinel-2B	2021-08-05	08WNU	Ascending	0.01	0.00	0.00
Sentinel-2B	2021-08-05	08WNV	Ascending	3.30	0.10	0.00
Sentinel-2B	2021-08-05	08WPU	Ascending	0.82	0.64	0.00
Sentinel-2B	2021-08-15	07WEM	Ascending	4.76	2.13	0.00
Sentinel-2A	2021-08-29	07WEN	Descending	2.91	2.29	0.00
Sentinel-2A	2021-08-30	08WPU	Ascending	3.87	1.58	0.00

SENTINEL-1 IMAGES

Sentinel-1 images were acquired as pre-processed Ground Range Detected, Interferometric Wide swath mode, Level 1 images in both VV and VH polarizations from Google Earth Engine. Interferometric Wide swath mode is the main acquisition mode over land and satisfies most project requirements, including wetland classification.

Table A2: List of Sentinel-1 Images used to Create the C-band SAR Mosaic for the Object-based Random Forest Classification

PLATFORM	SENSING DATE	ORBIT	IDENTIFIER
Sentinel-1A	2020-07-01	Ascending	S1A_IW_GRDH_1SDV_20200701T022313_20200701T022338_033255_03DA55_D82A
Sentinel-1A	2020-07-01	Ascending	S1A_IW_GRDH_1SDV_20200701T022338_20200701T022403_033255_03DA55_ACAA
Sentinel-1A	2020-07-01	Ascending	S1A_IW_GRDH_1SDV_20200701T022403_20200701T022428_033255_03DA55_8585
Sentinel-1A	2020-07-09	Ascending	S1A_IW_GRDH_1SDV_20200709T025616_20200709T025641_033372_03DDCA_F883
Sentinel-1A	2020-07-09	Ascending	S1A_IW_GRDH_1SDV_20200709T025641_20200709T025706_033372_03DDCA_18CB
Sentinel-1A	2020-07-11	Ascending	S1A_IW_GRDH_1SDV_20200711T023944_20200711T024009_033401_03DEBA_6463
Sentinel-1A	2020-07-11	Ascending	S1A_IW_GRDH_1SDV_20200711T024009_20200711T024034_033401_03DEBA_DFB4
Sentinel-1A	2020-07-11	Ascending	S1A_IW_GRDH_1SDV_20200711T024034_20200711T024059_033401_03DEBA_1B3E
Sentinel-1A	2020-07-13	Ascending	S1A_IW_GRDH_1SDV_20200713T022314_20200713T022339_033430_03DFA8_88B8
Sentinel-1A	2020-07-13	Ascending	S1A_IW_GRDH_1SDV_20200713T022339_20200713T022404_033430_03DFA8_5190
Sentinel-1A	2020-07-21	Ascending	S1A_IW_GRDH_1SDV_20200713T022404_20200713T022429_033430_03DFA8_A5E1
Sentinel-1A	2020-07-21	Ascending	S1A_IW_GRDH_1SDV_20200721T025617_20200721T025642_033547_03E328_0DC1
Sentinel-1A	2020-07-21	Ascending	S1A_IW_GRDH_1SDV_20200721T025642_20200721T025707_033547_03E328_FD4F
Sentinel-1A	2020-07-23	Ascending	S1A_IW_GRDH_1SDV_20200723T023945_20200723T024010_033576_03E41D_1CCC
Sentinel-1A	2020-07-23	Ascending	S1A_IW_GRDH_1SDV_20200723T024010_20200723T024035_033576_03E41D_76BD
Sentinel-1A	2020-07-25	Ascending	S1A_IW_GRDH_1SDV_20200723T024035_20200723T024100_033576_03E41D_B40F
Sentinel-1A	2020-07-25	Ascending	S1A_IW_GRDH_1SDV_20200725T022315_20200725T022340_033605_03E506_8FE2
Sentinel-1A	2020-07-25	Ascending	S1A_IW_GRDH_1SDV_20200725T022340_20200725T022405_033605_03E506_05F3

PLATFORM	SENSING DATE	ORBIT	IDENTIFIER
Sentinel-1A	2020-07-25	Ascending	S1A_IW_GRDH_1SDV_20200725T022405_20200725T022430_033605_03E506_FBD0
Sentinel-1A	2020-08-02	Ascending	S1A_IW_GRDH_1SDV_20200802T025618_20200802T025643_033722_03E88A_6A34
Sentinel-1A	2020-08-02	Ascending	S1A_IW_GRDH_1SDV_20200802T025643_20200802T025708_033722_03E88A_1D1D
Sentinel-1A	2020-08-04	Ascending	S1A_IW_GRDH_1SDV_20200804T023946_20200804T024011_033751_03E972_1B9B
Sentinel-1A	2020-08-04	Ascending	S1A_IW_GRDH_1SDV_20200804T024011_20200804T024036_033751_03E972_3214
Sentinel-1A	2020-08-06	Ascending	S1A_IW_GRDH_1SDV_20200804T024036_20200804T024101_033751_03E972_C1D7
Sentinel-1A	2020-08-06	Ascending	S1A_IW_GRDH_1SDV_20200806T022316_20200806T022341_033780_03EA71_7C69
Sentinel-1A	2020-08-06	Ascending	S1A_IW_GRDH_1SDV_20200806T022341_20200806T022406_033780_03EA71_F45E
Sentinel-1A	2020-08-06	Ascending	S1A_IW_GRDH_1SDV_20200806T022406_20200806T022431_033780_03EA71_390C
Sentinel-1A	2020-08-14	Ascending	S1A_IW_GRDH_1SDV_20200814T025618_20200814T025643_033897_03EE6C_EC69
Sentinel-1A	2020-08-14	Ascending	S1A_IW_GRDH_1SDV_20200814T025643_20200814T025708_033897_03EE6C_68CF
Sentinel-1A	2020-08-16	Ascending	S1A_IW_GRDH_1SDV_20200816T023946_20200816T024011_033926_03EF7D_EDA3
Sentinel-1A	2020-08-16	Ascending	S1A_IW_GRDH_1SDV_20200816T024011_20200816T024036_033926_03EF7D_8271
Sentinel-1A	2020-08-16	Ascending	S1A_IW_GRDH_1SDV_20200816T024036_20200816T024101_033926_03EF7D_721B
Sentinel-1A	2020-08-18	Ascending	S1A_IW_GRDH_1SDV_20200818T022316_20200818T022341_033955_03F08E_5E37
Sentinel-1A	2020-08-18	Ascending	S1A_IW_GRDH_1SDV_20200818T022341_20200818T022406_033955_03F08E_F09C
Sentinel-1A	2020-08-18	Ascending	S1A_IW_GRDH_1SDV_20200818T022406_20200818T022431_033955_03F08E_6DB0
Sentinel-1A	2020-08-28	Ascending	S1A_IW_GRDH_1SDV_20200828T023947_20200828T024012_034101_03F5A5_9A5F
Sentinel-1A	2020-08-28	Ascending	S1A_IW_GRDH_1SDV_20200828T024012_20200828T024037_034101_03F5A5_2C35
Sentinel-1A	2020-08-28	Ascending	S1A_IW_GRDH_1SDV_20200828T024037_20200828T024102_034101_03F5A5_4363
Sentinel-1A	2020-08-30	Ascending	S1A_IW_GRDH_1SDV_20200830T022317_20200830T022342_034130_03F6BA_0F67
Sentinel-1A	2020-08-30	Ascending	S1A_IW_GRDH_1SDV_20200830T022342_20200830T022407_034130_03F6BA_D915
Sentinel-1A	2020-08-30	Ascending	S1A_IW_GRDH_1SDV_20200830T022407_20200830T022432_034130_03F6BA_FE49

ALOS PALSAR IMAGES

ALOS PALSAR images were acquired as pre-processed Fine Bean Dual mode images in both HH and HV polarizations from the Alaska Satellite Facility (see https://asf.alaska.edu/).

Table A3: List of ALOS PALSAR Images used to Create the L-band SAR Mosaic for the Object-based Random Forest Classification

PLATFORM	SENSING DATE	ORBIT	GRANULE	PATH	FRAME
ALOS	2010-08-27	Ascending	ALPSRP244511340	24451	235
ALOS	2010-08-27	Ascending	ALPSRP244511330	24451	235
ALOS	2010-08-27	Ascending	ALPSRP244511320	24451	235
ALOS	2010-08-27	Ascending	ALPSRP244511310	24451	235
ALOS	2010-08-27	Ascending	ALPSRP244511300	24451	235
ALOS	2010-08-27	Ascending	ALPSRP244511290	24451	235
ALOS	2010-08-27	Ascending	ALPSRP244511280	24451	235
ALOS	2010-08-22	Ascending	ALPSRP243781340	24378	232
ALOS	2010-08-22	Ascending	ALPSRP243781330	24378	232
ALOS	2010-08-22	Ascending	ALPSRP243781320	24378	232

PLATFORM	SENSING DATE	ORBIT	GRANULE	PATH	FRAME
ALOS	2010-08-22	Ascending	ALPSRP243781310	24378	232
ALOS	2010-08-22	Ascending	ALPSRP243781300	24378	232
ALOS	2010-08-22	Ascending	ALPSRP243781290	24378	232
ALOS	2010-08-22	Ascending	ALPSRP243781280	24378	232
ALOS	2010-08-17	Ascending	ALPSRP243051320	24305	229
ALOS	2010-08-17	Ascending	ALPSRP243051310	24305	229
ALOS	2010-08-17	Ascending	ALPSRP243051300	24305	229
ALOS	2010-08-17	Ascending	ALPSRP243051290	24305	229
ALOS	2010-08-17	Ascending	ALPSRP243051280	24305	229
ALOS	2010-08-15	Ascending	ALPSRP242761340	24276	237
ALOS	2010-08-15	Ascending	ALPSRP242761330	24276	237
ALOS	2010-08-15	Ascending	ALPSRP242761320	24276	237
ALOS	2010-08-15	Ascending	ALPSRP242761310	24276	237
ALOS	2010-08-15	Ascending	ALPSRP242761300	24276	237
ALOS	2010-08-15	Ascending	ALPSRP242761290	24276	237
ALOS	2010-08-15	Ascending	ALPSRP242761280	24276	237
ALOS	2010-08-05	Ascending	ALPSRP241301340	24130	231
ALOS	2010-08-05	Ascending	ALPSRP241301330	24130	231
ALOS	2010-08-05	Ascending	ALPSRP241301320	24130	231
ALOS	2010-08-05	Ascending	ALPSRP241301310	24130	231
ALOS	2010-08-05	Ascending	ALPSRP241301300	24130	231
ALOS	2010-08-05	Ascending	ALPSRP241301290	24130	231
ALOS	2010-08-05	Ascending	ALPSRP241301280	24130	231
ALOS	2010-08-03	Ascending	ALPSRP241011340	24101	239
ALOS	2010-08-03	Ascending	ALPSRP241011330	24101	239
ALOS	2010-08-03	Ascending	ALPSRP241011320	24101	239
ALOS	2010-08-03	Ascending	ALPSRP241011310	24101	239
ALOS	2010-08-03	Ascending	ALPSRP241011300	24101	239
ALOS	2010-08-03	Ascending	ALPSRP241011290	24101	239
ALOS	2010-08-03	Ascending	ALPSRP241011280	24101	239
ALOS	2010-07-26	Ascending	ALPSRP239841340	23984	225
ALOS	2010-07-26	Ascending	ALPSRP239841330	23984	225
ALOS	2010-07-26	Ascending	ALPSRP239841320	23984	225
ALOS	2010-07-26	Ascending	ALPSRP239841310	23984	225
ALOS	2010-07-26	Ascending	ALPSRP239841300	23984	225
ALOS	2010-07-26	Ascending	ALPSRP239841290	23984	225
ALOS	2010-07-26	Ascending	ALPSRP239841280	23984	225
ALOS	2010-07-21	Ascending	ALPSRP239111340	23911	222
ALOS	2010-07-21	Ascending	ALPSRP239111330	23911	222
ALOS	2010-07-21	Ascending	ALPSRP239111320	23911	222

PLATFORM	SENSING DATE	ORBIT	GRANULE	PATH	FRAME
ALOS	2010-07-21	Ascending	ALPSRP239111310	23911	222
ALOS	2010-07-21	Ascending	ALPSRP239111300	23911	222
ALOS	2010-07-21	Ascending	ALPSRP239111290	23911	222
ALOS	2010-07-04	Ascending	ALPSRP236631340	23663	221
ALOS	2010-07-04	Ascending	ALPSRP236631330	23663	221
ALOS	2010-07-04	Ascending	ALPSRP236631320	23663	221
ALOS	2010-07-04	Ascending	ALPSRP236631310	23663	221
ALOS	2010-07-02	Ascending	ALPSRP236341340	23634	229
ALOS	2010-07-02	Ascending	ALPSRP236341330	23634	229
ALOS	2008-08-23	Ascending	ALPSRP137441340	13744	227
ALOS	2008-08-23	Ascending	ALPSRP137441330	13744	227
ALOS	2008-08-23	Ascending	ALPSRP137441320	13744	227
ALOS	2008-08-23	Ascending	ALPSRP137441310	13744	227
ALOS	2008-08-23	Ascending	ALPSRP137441300	13744	227
ALOS	2008-08-23	Ascending	ALPSRP137441290	13744	227
ALOS	2008-08-23	Ascending	ALPSRP137441280	13744	227
ALOS	2008-08-04	Ascending	ALPSRP134671300	13467	234
ALOS	2008-08-04	Ascending	ALPSRP134671290	13467	234
ALOS	2008-08-04	Ascending	ALPSRP134671280	13467	234
ALOS	2008-08-01	Ascending	ALPSRP134231340	13423	223
ALOS	2008-08-01	Ascending	ALPSRP134231330	13423	223
ALOS	2008-08-01	Ascending	ALPSRP134231320	13423	223
ALOS	2008-08-01	Ascending	ALPSRP134231310	13423	223
ALOS	2008-08-01	Ascending	ALPSRP134231300	13423	223
ALOS	2008-08-01	Ascending	ALPSRP134231290	13423	223
ALOS	2008-08-01	Ascending	ALPSRP134231280	13423	223

Appendix B

Supplemental Assessments of Classification Accuracy

SUPPLEMENTAL PIXEL-BASED ASSESSMENTS

Table B1: The Overall, Producer, and User Accuracies of Wetland and Non-wetland Classes, Calculated Through a Pixel-based Assessment, within the Areas of Special Interest

OVERALL ACCURACY: 96.55%	KAPPA COEFFICIENT: 0.93	USER ACCURACY (%)
CLASS	PRODUCER ACCURACY (%)	
Wetland Class		
Shallow water	89.88	83.45
Marsh	68.81	54.18
Fen	79.44	89.72
Bog	85.39	91.77
Swamp	69.92	44.96
Non-wetland Class		
Deep water	98.94	92.10
Exposed/disturbed	64.57	96.23
Coniferous forest	86.18	89.66
Broadleaf forest	57.28	61.83
Shrubland	69.59	30.82

Table B2: Confusion Matrix Obtained Based on the Produced Classification Calculated on a Per Pixel Basis for the Entire Mayo and McQuesten Watersheds

		REFERENCE SAMPLES (PERCENT OF PIXELS)									
		DEEP WATER	SHALLOW WATER	MARSH	FEN	BOG	SWAMP	EXPOSED/ DISTURBED	CONIFEROUS	BROADLEAF	SHRUBLAND
MAPPED CLASS	Deep Water	98.94	8.16	0.19	0.00	0.00	0.03	0.02	2.95	0.03	0.04
	Shallow Water	0.94	89.88	2.83	0.01	0.02	0.00	0.00	0.00	0.00	0.00
	Marsh	0.09	0.76	68.81	0.89	0.35	5.26	0.00	0.22	0.01	0.00
	Fen	0.02	0.76	26.80	79.44	11.1	3.83	0.00	1.47	0.02	8.16
	Bog	0.00	0.00	0.05	0.23	85.39	0.00	0.00	2.93	0.00	0.00
	Swamp	0.00	0.00	0.15	3.41	0.00	69.92	0.00	1.79	23.28	0.00
	Exposed/ Disturbed	0.02	0.00	0.00	0.4	0.00	0.10	64.57	0.57	0.05	6.45
	Coniferous	0.00	0.45	0.39	0.95	2.18	10.71	0.05	86.18	11.38	3.74
	Broadleaf	0.00	0.00	0.00	0.00	0.00	4.31	0.00	0.76	57.28	12.01
	Shrubland	0.00	0.00	0.78	14.66	0.96	5.84	35.36	3.12	7.94	69.59

Table B4: The Overall, Producer, and User Accuracies of Wetland and Non-wetland Classes, Calculated Through an Object-based Assessment

OVERALL ACCURACY: 80.87%	KAPPA COEFFICIENT: 0.76	USER ACCURACY (%)
CLASS	PRODUCER ACCURACY (%)	
Wetland Class		
Shallow Water	77.78	77.78
Marsh	60.71	65.38
Fen	85.50	86.36
Bog	85.71	90.41
Swamp	50.00	82.14
Non-wetland Class		
Deep water	95.24	83.33
Exposed/disturbed	96.70	93.18
Coniferous forest	76.52	73.33
Broadleaf forest	78.05	72.72
Shrubland	68.57	64.28

Table B5: Confusion Matrix for Wetland and Non-Wetland Classes Calculated on a Per Object Basis

MAPPED CLASS	REFERENCE SAMPLES (PERCENT OF PIXELS)									
	DEEP WATER	SHALLOW WATER	MARSH	FEN	BOG	SWAMP	EXPOSED/ DISTURBED	CONIFEROUS	BROADLEAF	SHRUBLAND
Deep Water	20	2	–	–	–	–	–	2	–	–
Shallow Water	1	7	1	–	–	–	–	–	–	–
Marsh	–	–	17	3	1	2	–	1	1	1
Fen	–	–	8	171	6	5	–	2	–	6
Bog	–	–	–	3	66	-	–	4	–	–
Swamp	–	–	–	–	–	23	–	5	–	–
Exposed/ Disturbed	–	–	–	3	–	–	205	4	–	8
Coniferous	–	–	–	5	2	9	1	88	5	10
Broadleaf	–	–	–	–	–	2	–	2	32	8
Shrubland	–	–	2	15	2	5	6	7	3	72